NATIONAL BUREAU OF STANDARDS REPORT

8147

EXPERIMENTAL FIRES IN ENCLOSURES

by

D. Gross
and
A. F. Robertson

U. S. DEPARTMENT OF COMMERCE
NATIONAL BUREAU OF STANDARDS

NATIONAL BUREAU OF STANDARDS REPORT

NBS PROJECT		NBS REPORT
1002-11-10122	December 12, 1963	8147

EXPERIMENTAL FIRES IN ENCLOSURES

by

D. Gross

and

A. F. Robertson

U. S. DEPARTMENT OF COMMERCE
NATIONAL BUREAU OF STANDARDS

EXPERIMENTAL FIRES IN ENCLOSURES

by

D. Gross
and
A. F. Robertson

Abstract

Results are presented of experimental measurements of the mass rates of burning, temperatures and gas compositions in model enclosures of three sizes. Interest was confined to the fully-developed period of burning in which the burning rate of a combustible fiberboard crib was limited by the size and shape of the ventilation opening. The burning rate was found to be generally proportional to $A\sqrt{h}$ (A=area, h=height of window opening), but a characteristic transition region was found for each enclosure which resulted in an abrupt shift in the data line. Burning rate data were correlated in terms of the ventilation parameter $A\sqrt{h}$ and the exposed surface area of the crib.

The overall process involved in enclosure fires appears to be a combined gravity-controlled fluid dynamic regime and a radiation-controlled thermal regime. The dimensionless Froude group is the criterion for similarity in a gravity- (buoyancy-) controlled regime, and from the limited agreement found among the data for the two larger enclosures, this group appears to include the essential parameters in the scaling of burning rates of fires in geometrically similar enclosures.

EXPERIMENTAL FIRES IN ENCLOSURES

by

D. Gross
and
A. F. Robertson

1. Introduction

The analysis of fires in rooms, buildings and full-size structures is admittedly complex due to the interaction of mechanical, diffusional, thermal and chemical processes. Although the same interactions complicate experimentation and analysis on small-scale models, the use of models permits a great many more experiments to be performed under more controllable conditions.

As part of a program to develop basic information on the use of models in fire research, exploratory experimental measurements were made of the mass rates of burning, temperatures and gas compositions in model enclosures. Interest was mainly confined to the fully-developed stages of fires in which the ventilation opening limited the burning rate of a reproducible crib-type combustible load [1]. The data supplement other published information on fire behavior in both model [2, 3, 4] and full-scale [5, 6] enclosures and permit consideration of appropriate scaling relationships. One ultimate objective is the use of models to evaluate the degree of hazard when flames spread along the surfaces of flammable interior finish materials in enclosures.

2. Test Procedures and Equipment

In this series, experiments were limited to geometrically similar(1:1:2) box-type enclosures of three sizes containing (usually) only a single rectangular ventilation opening. Several tests with dual windows were also made. Size and construction details are summarized in Table 1. Fig. 1 is a schematic diagram of the experimental apparatus. A cellulose-base fiberboard was used as the crib material because of its rapid flaming characteristics, and the cribs were constructed so that the spacing between sticks was three times the stick width. The sticks were of square cross-section and, except for selected tests, were 2.5 cm thick for the Scale I and II model enclosures and 7.5 cm thick for the Scale III model enclosure. Except as noted later, the crib for the two smaller enclosures were of very nearly identical weight and construction and averaged approximately 270 g and 3200 g, respectively, for the Scale I and Scale II enclosure tests.

The crib was supported from 1 to 3 stick widths above the enclosure floor and was located between the center and rear of the box. The test was started by igniting kerosene-soaked fiberboard wicks placed in the openings of the bottom row of sticks. Temperatures were measured at several locations within the box by means of chromel-alumel thermocouples made of 0.051 cm dia. wires with asbestos and glass, silicone-impregnated insulation and bare, unshielded beads. Temperatures were automatically recorded on a multipoint potentiometer recorder.

Gas composition measurements were made using an uncooled probe made of 1/4 in. o.d. copper tubing placed at the top front of the burning crib. All gas compositions were assumed "dry." Moisture and other condensable combustion products were removed prior to measurement by passing the sample through the following, in order: (1) a glass fiber filter, tar and resin trap, (2) an ice-cooled moisture and liquid trap, (3) two air line filters in series prior to the vacuum pump, and (4) one air line filter after the vacuum pump. All instruments were operated above room temperature. The gas sampling arrangement is shown schematically in Fig. 2.

The analyzers used for CO and CO_2 were Model 300 "Lira" Infrared Analyzers, manufactured by Mine Safety Appliances Co. These instruments analyze an unknown gas by comparing its infrared absorption quality with the constant infrared absorption quality of a known gas. This is accomplished by alternate interruption of infrared radiation beams through the unknown sample gas and the known comparison gas causing a differential response by a single sealed-in detector gas which is related to the volume fraction of the desired component. These instruments had full-scale ranges of 0-14 percent CO and 0-20 percent CO_2, had a response speed of 5 seconds (to 90% of final reading), and a rated accuracy of ± 2 percent of full scale. For oxygen determinations a Model F3 Oxygen Analyzer manufactured by Beckman Instruments, Inc., was used. Here the very high magnetic susceptibility of oxygen is employed to rotate a quartz fiber suspension system and the rebalance potential is a direct and proportional measure of the oxygen content of the sample gas. The instrument had a full-scale range of 0-25 percent oxygen.

All instruments were standardized at their zero points with commercial high-purity nitrogen and at or close to their span points with instrument calibration mixtures. Electrical output signals from all instruments were recorded continuously on balancing potentiometer-type recorders.

3. Discussion of Results

Rate of Burning. The rate of burning of the crib, r, was taken as the mean rate of weight loss from 80 percent to 30 percent of the original crib weight and expressed in g/sec. As illustrated by the typical weight-time curve in Fig.3, a fairly uniform rate of burning occurs during this period which corresponds to the fully developed stage of burning. These average burning rates have been plotted in terms of a ventilation parameter, $A\sqrt{h}$, where A and h are the area and height of the window opening, respectively. Considering that the velocity of non-viscous flow through an orifice is proportional to the square root of its height, the ventilation parameter may be taken to represent the total induced air flow through the opening. (See Fig. 4) Test results for all three enclosures are summarized in Table 2 and plotted in Fig. 5. It may be observed that for each of the two smaller enclosures and the corresponding crib weight, a limiting value of $A\sqrt{h}$ was reached beyond which the window no longer limited, and the rate of burning had a constant value equal (very nearly) to the rate of burning of the crib in the open.

For each enclosure, the date for the vertical and horizontal windows are in close agreement. This means that a rectangular vertical window will permit burning at a greater rate than a horizontal window of equal area. However, a slight variation in this trend was noticed above the transition zone for the Scale II enclosure and this may be noted from the data points inFig. 5. Results with two horizontal windows located at top and bottom are also included and suggest that the effective height for multiple windows extends from the bottom of the lowest low-level opening to the top of the highest high-level opening with an increased effective velocity.

A characteristic transition region was found for each enclosure in which the data line for small window openings was shifted upward. The data for this line has been extended to include extermely small openings where an essentially pyrolytic reaction was occurring with the absence of visible flaming. In such cases, repeated and prolonged ignition was required to elevate the enclosure temperature to that required for sustaining the pyrolysis. This transition region appears to be associated with (1) a characteristic change in the position of flaming from predominantly within the crib to regions of more ready access of oxygen, and (2) a corresponding change in the fraction of the window opening used for inducing air into the enclosure.

For the Scale II and Scale III enclosures, the mean value of the ratio between r and $a\sqrt{h}$ is approximately 0.0015 g/sec $cm^{5/2}$ in fair agreement with the overall average value of 0.001 g/sec $cm^{5/2}$ (6 kg/min $m^{5/2}$) summarized by Thomas [2] for fires in model and full-size enclosures burning wood fuel.

Surface Area. As indicated under Test Procedure, cribs of identical weight, construction and exposed surface area were used for the bulk of the tests in each of the Scale I and Scale II enclosures, whereas some weight (and surface area) variations were used in the Scale III enclosure. Additional tests were subsequently performed in the Scale II enclosures using cribs of varying weights and surface areas, and in the Scale III enclosure in which equal weight cribs, but of different surface areas were used (at the same $A\sqrt{h}$). The results indicated that, for a ventilation-limited enclosure, the mean rate of burning could be related to the exposed surface area of the crib, as shown in Figs. 6a, b, and c. The data for the Scale III enclosure (Fig. 6c) group together nicely when surface area variations are thus accounted for.

The visually estimated "best fit" lines for the three enclosures have been redrawn in Fig. 7, from which it may be noted that, despite a definite pattern of differences between the scales, a general overall concordance was found to exist. The lines for the Scale II and Scale III enclosures are of unit slope in conformance with a direct proportionality, whereas the data for the Scale I enclosure indicates a power relationship. The maximum burning rate was approximately 0.0007 g/sec cm^2 for all scale sizes, and the location of the transition region corresponded to a value for $A\sqrt{h}/A_s$ of approximately 0.1 $cm^{1/2}$.

The effect of stick spacing on the rate of burning was only explored for a single ventilation condition in the Scale II enclosure and with a different fiberboard. The comparative results are given in Table 3. Although these tests should not be considered conclusive, it appears as if the spacing chosen as standard for the overall test series (i.e. a spacing of 3 stick widths) may not result in the maximum rate of burning such as would be the case for burning in the open [7].

It should be emphasized that these results may apply only to the enclosure configuration and construction and location of crib studied, and that caution should be exercised in trying to apply the data to other situations.

Temperature. Thermocouple temperature measurements near the upper edge of the crib were averaged over the time period corresponding to the 80 to 30 percent weight loss and are plotted in Fig. 8. For each enclosure, the average temperature increased with $A\sqrt{h}/A_s$, but tended to level out for the largest window openings. There was an upward shift in temperature from the smallest to the largest size enclosure.

It is realized that a bare, unshielded thermocouple placed in a chamber in which the gases and walls are not at the same temperature will not give a true indication of the gas temperature. The magnitude of the radiation error introduced depends upon the temperatures, the surface heat transfer coefficient, the size (surface area) of the thermocouple bead, and its emissivity. Under the test conditions and temperatures, the radiation errors [8] are generally less than about 5 percent of the absolute temperature (or less than 80°C) and no effect on the conclusions drawn are expected by such variations. No radiation measurements were made.

Gas Composition. Gas composition measurements at the top front of the burning crib were assumed representative of the gases generated by the combustion with a minimum of dilution and mixing effects. Check traverses which indicate the approximate changes in gas composition due to flow patterns and mixing are shown in Fig. 9 for the Scale II enclosure.

The mole percent gas composition measurements for the Scale II and Scale III enclosures were also averaged over the time period corresponding to the 80 to 30 percent weight loss. As shown in Fig. 10, the general trends were similar and shifts corresponding to the transition regions were noticed, particularly for the Scale III enclosure. The percentages of CO and CO_2 the Scale III enclosure were slightly lower (and more variable) than the corresponding values in the Scale II enclosure. This may have resulted from a different pattern of flow and mixing in the two enclosures, since care was taken to locate the sampling tubes in geometrically similar positions.

The CO percentage increased with the ventilation parameter for both the Scale II and Scale III enclosures whereas O_2 concentration decreased and generally remained at or below 1 percent for window openings for which active flaming was observed, $A\sqrt{h}/A_s = 0.06$ $cm^{1/2}$ approximately. At this ventilation also, the CO_2 concentration increased and remained above 18 percent for all larger window openings in the Scale II enclosure and generally above 16 percent in the Scale III enclosure. The data for the two largest ventilation openings in the Scale III enclosure appear to be anomolous (presumably due to insufficient load for the burning to be considered ventilation-limited) and have not been plotted in Fig. 10.

Neutral Zone and Velocity Measurements. In order to determine the volumetric flow rate of exhaust products, attempts were made to measure the position of the neutral zone and the velocity profile across the window opening as described by Van Arsdale [19].

The optical distortion technique used for neutral zone determinations depends upon the difference in the densities and hence the refractive indices of the cool and hot gases at the neutral zone boundary. By placing a grid of white lines on a black background behind the plane of the enclosure window, the displacement or distortion of the grid lines by the hot gases and flames may be photographically recorded. Based upon a limited number of tests with the Scale II enclosure, it was concluded (1) that the boundary height shifted periodically during each test, with the frequency of oscillation related inversely to $A\sqrt{h}$, whereas the amplitude of oscillation was greatest at $A\sqrt{h}$ values corresponding to the transition region, and (2) that, except for the transition region, the mean height of the neutral zone boundary increased with $A\sqrt{h}$.

For measuring velocities of the hot exiting gases, a flow visualization technique involving interrupted streak photography of low density perlite particles was used. As shown schematically in Fig. 11, the perlite particles (preferably those in the 75 to 150 micron size range) were injected along the optical axis of the camera, the direction in which the flowing gases have no velocity component. Illumination was provided by four large flash bulbs located in a hooded parabolic trough beneath the enclosure opening, which projected a narrow (2-in.) band of light upward. Sufficient illumination intensity was required to show up the particles against the intensity of the flame and against the incandescence of the particles themselves. The flash bulbs (Sylvania type 2A) were triggered in sequence in order to extend the illuminated period to about 0.2 sec. Light reflected from the particles was periodically interrupted by a rotating flat-bladed fan, with two 30-degree blades, driven by an 1800 rpm constant speed motor, providing a light period of 1/72 second followed by a dark period of 1/360 second. Difficulties with clogging of the perlite in the dispensing tubes (despite the use of vibrators and air pressure) did not permit a reliable constant flow dispersion of perlite particles to be achieved. Nevertheless, the interrupted streak technique for velocity measurement still appears feasible, and would be extremely useful if combined with simultaneous photographic recording of the neutral zone boundary.

4. Analysis

Combustion Reactions and Products. The decomposition of a complex carbohydrate fuel into elementary fuels -- carbon, gaseous hydrocarbons, carbon monoxide and hydrogen -- is considered to occur prior to the start of actual combustion. Analysis of basic combustion reactions may therefore be an aid in the interpretation of cellulose burning and the associated heat and mass flow balances.

If we consider that the normal product of combustion of cellulose burning is CO_2 and that part of it is reduced to CO, the extent of this secondary reaction will be dependent upon the relative amounts of cellulose (carbon) and oxygen, the time of contact between the initially formed CO_2, the reactivity of the (carbon) surface and the temperature [10].

Many theories have been postulated for the type and sequence of reactions involved in the combustion of carbon and of cellulose. However, whatever the theory, the net heat liberated by combustion is determined by the ratio of CO to CO_2 in the products [11]. In fact, a measure of the effectiveness of glow retardants is the resultant increase in the $CO:CO_2$ ratio of the products and minimization of the heat available for propagating the oxidation.

The following analysis is similar to that outlined extensively by Kawagoe [5] but is based upon the measured exhaust gas compositions and has been carried through on a molar basis.

Assuming the fuel to consist of pure dry cellulose, $C_6H_{10}O_5$, a simplified equation for the combustion reaction would be:

$$C_6H_{10}O_5+(3+3x+f)\ O_2+\frac{79}{21}(3+3x+f)N_2 \longrightarrow 6xCO_2+6(1-x)CO+5H_2O+fO_2+\frac{79}{21}(3+3x+f)N_2$$

where $x=\frac{[CO_2]}{[CO]+[CO_2]}$ is the fraction of complete combustion,

i.e., the fraction of the fuel carbon which is converted to CO_2 (expressed in terms of the mole volumes of the products), and f, the uncombined oxygen factor is equal to the moles of oxygen in the products. The value of f may be determined from the relation:

$$[O_2] = \frac{f}{6+5+f+\frac{79}{21}(3+3x+f)} \quad .$$

The combustion reaction equation assumes that all fuel carbon is converted to CO and CO_2 (none is dispersed as soot) and that all the fuel hydrogen appears as water vapor. Each mole of cellulose produces a total of six moles of CO and CO_2 irrespective of the relative percentages of each.

With complete combustion, the theoretical minimum anount of air required would be 6 moles, so that the quantity

$$n = \frac{3+3x+f}{6}$$

is defined as the excess air factor and has a value of 1 when $x = 1$ and $f = o$, corresponding to complete combustion with no excess air.

It is evident that for a carbon fuel, the combined CO_2 plus O_2 is 21% by volume (on a dry basis) and that a CO_2 percentage of 21 represents no excess air while a smaller CO_2 percentage represents an excess of air. As the hydrogen content of the fuel increases, the volume percent of CO_2 plus O_2 decreases. Likewise, the presence of O_2 ($f>0$) represents excess air and its absence no excess air. The two conditions should occur simultaneously; however, the CO percentage depends upon both temperature (especially with excess air) and the availability of oxygen (i.e. without excess air). The presence of CO together with O_2 at low temperatures (small openings) is not unusual--it actually represents complete combustion for the existing temperature.

At any given temperature (and pressure), a reaction will not proceed completely in either direction, although equilibrium may usually be very far in the direction of complete combustion. At ordinary temperatures (< 1500°K) for example, the reaction $2CO + O_2 \longrightarrow 2CO_2$ goes to completion with no O_2 or CO in equilibrium. In the presence of carbon (charcoal) and absence of oxygen, however, the governing reaction probably approaches $C + CO_2 \longrightarrow 2CO$, for which the temperature-equilibrium composition [10, 12] as shown in Fig. 12.

For comparison, the equilibrium composition for the gas-phase reactions $CO + H_2O \rightleftharpoons CO_2 + H_2$ and $2\ CO + O_2 \longrightarrow 2\ CO_2$ are also shown. As can be seen, the measured CO/CO_2 ratios for the Scale II enclosure tend to increase slightly with the measured temperature at the probe inlet. However, the agreement with the predicted equilibrium mixture in the presence of carbon is not particularly good, and extreme deviations occur at temperatures above 675°C. It is evident that in an open system such as this with the possibility of continuing reactions occurring in the sampling tube (where carbon is no longer present), the assumption of equilibrium conditions and a single simple reaction is inappropriate.

Since the overall reaction: Cellulose + $O_2 \longrightarrow CO_2 + CO + H_2O$ is very rapid at the high temperatures involved in flaming gas phase combustion, but is relatively slow below 200°C, cooling of the products should produce a "frozen equilibrium" condition in which very little change should occur in the proportions of the different gases. As previously stated, gas composition measurements for this exploratory study were made using an uncooled probe. The sampling rate was maintained at 2500 cc/min to satisfy the requirements of the gas analysis instruments. In a check measurement, a water-cooled probe was located in close proximity to the uncooled probe and alternate samplings were made from each probe. Gas samples were also withdrawn and analyzed by means of a mass spectrometer. The average values of the two sets of measurements, listed in Table 4, show significant composition changes with and without probe cooling. However, the CO/CO_2 ratio was not affected to anywhere near the same extent. This data is also shown in Fig. 12.

In a study of sampling of hot combustion gases from a controlled Bunsen-type methane flame, it was found that both rate of sampling and probe size had a small but noticeable effect on sample composition [13]. It was also determined that the water-cooled probes used were unable to quench the reactions completely, but that the lower the temperature of the gas being sampled, the more effective was the quenching. The "apparent quenching temperature" (2200-2500 K) based upon CO/CO_2 and H_2/H_2O ratios was found to be considerably below the calculated flame temperature (2800 K) for one methane mixture used. Extrapolation of data for several mixtures led to the conclusion that the "apparent quenched temperature"

would appear to coincide with the calculated flame temperature at about 1600°K and thus at this temperature, a probe should function perfectly and the composition of the cooled gas should be the same as the composition of the flame gas. Due to dilution and mixing, the maximum measured temperatures in the model enclosure tests never exceeded 1600°K.

Variations in the value of x, the fraction of complete combustion, is shown for the Scale II and III enclosures in Fig. 13.

Similarity Considerations. In order to enhance the usefulness of the data presented, an attempt was made toward understanding and establishing appropriate similarity criteria for combustion reactions in restricted ventilation enclosures.

From the basic chemistry of cellulose burning and consideration of fluid flow through an opening, Kawagoe [5] showed that the fuel combustion rate r could be expressed as a function of the coefficient of discharge C, the opening area A, the effective height of the opening h, the temperature difference between the enclosure and the surroundings, and the volume of exhaust gas per unit weight of fuel G, as follows:

$$r \propto \frac{C\sqrt{\frac{\Delta T}{To}}\, A\sqrt{h}}{G}$$

G is a function of the temperature T in the box, the fraction of complete combustion, x, and the amount of excess air, n. It may be noted that, using an appropriate density (ρ), the quantity $\frac{r}{\rho CA\sqrt{\frac{\Delta T}{To}\, h}}$ may be considered a dimensionless fuel to air ratio. The effective height of the opening is determined by the location of a neutral zone, which is the horizontal level at which no pressure difference and hence no flow exists. This is shown schematically in Fig. 4.

The significance of the neutral zone in building ventilation was described by Emswiler [14] who considered multiple openings in a structure and illustrated the computation of air flow in terms of temperature difference and Bernoulli's equation. Recently, Brown and Solvason [15] presented a generalized theory of natural convection across single and

multiple openings in vertical partitions. For ventilation problems, it may be assumed that density differences are small compared with the mean density, and that vertical temperature gradients do not seriously alter the flow conditions. However, for flows involving flames and hot combustion products, the consideration of the effects of large temp. gradients is necessary.

It appears as if the overall process is a combined gravity-controlled fluid dynamic regime and a radiation-controlled thermal regime. In the latter regime, for geometrically similar systems of different sizes, the radiation group (bulk transport/radiation) and the Peclet group (bulk transport to conduction) are the conditions for similarity and are generally incompatible. However, since conduction is important only insofar as it affects the loss of heat through the boundary walls, similarity with respect to radiation and bulk transport may be attained. The similarity conditions for systems at the same temperature require that both the fluid velocities and the conducted heat loss per unit area of wall be made equal in model and prototype. For steady-state conditions, the latter is satisfied if the walls are made of the same material of the same thickness (or have the same ratio of thickness to thermal conductivity) and are subjected to the same temperature difference.

As with burning cross-piles of wood in the open, the dimensionless Froude group is the criterion for similarity in a gravity (buoyancy) controlled regime [7]. The modified Froude number based on buoyancy is defined as

$$N_{FR} = \left(\frac{\rho_1}{\rho_o - \rho_1} \right) \frac{v^2}{gh}$$

where ρ_o and p_1 are the densities of the cold air and the hot product gases respectively, v is the effective gas velocity, and h is the characteristic height determining buoyancy (here taken as the window height). The velocity may be determined from the following relation between the volume of products formed per unit fuel weight G, the effective exhaust area (assumed constant and equal to A/2), and the mean rate of burning r:

$$v = \frac{2\ Gr}{A}$$

The modified Froude number may therefore be written:

$$N_{FR} = \left(\frac{\rho_1}{\rho_o - \rho_1} \right) \frac{\left(\frac{2Gr}{A}\right)^2}{gh} = \frac{4}{g} \left(\frac{T_o}{T_1 - T_o} \right) \frac{G^2 r^2}{A^2 h}$$

The volume of gases produced (G) will depend upon the temperature, the amount of excess air and the extent to which combustion is complete. The value of G for cellulose containing 13 percent moisture is given both graphically and in tabular form by Kawagoe [5] or, for pure dry cellulose, may be computed from the relation

$$G = \frac{T+273}{273} \quad (1.07 + 3.98n - 0.406x) \; .10^3 \quad cm^3/g$$

For those tests in the Scale II and Scale III enclosures for which gas composition and temperature measurements were available, the values of G and N_{FR} have been computed and these are listed in Table 2. Figure 14 indicates the change in Froude number as a function of $A\sqrt{h}/A_s$. Despite considerable scatter, it may be seen that there is the general tendency for N_{FR} to decrease with increased $A\sqrt{h}/A_s$. A Froude number of 1 indicates equal inertia and buoyancy forces, so that buoyancy tends to predominate at higher values of $A\sqrt{h}/A_s$. The characteristic shift at the transition zone is not nearly as pronounced as in the burning rate curves, perhaps an indication of the appropriateness of the Froude number grouping in accounting for the observed chemical and physical changes in the burning behavior.

Heat Balance. Considering that 5 moles of water vapor are formed from the burning of 1 mole of cellulose, the measured CO, CO_2, and O_2 volume percentages were converted from a dry to a wet basis and an estimation made of the heat content (enthalpy) of the product gases. The mole fraction of water vapor was obtained from the ratio $\frac{5}{6+5+f+\frac{79}{21}(3+3x+f)}$. The heat content values for the gases CO_2, CO, O_2, H_2O, and N_2 at the measured temperatures [16] are listed for a typical case in Table 5.

Since the mole ratio of exhaust products to cellulose is equal to $6 + 5 + f + 79/21 (3 + 3x + f) = 31.8$, the net heat content of the exhaust products is equal to $31.8 (9.18 - 2.14) = 224$ kcal/mole of cellulose. The corresponding net heat of combustion, from the relation $219.4 + 405.6 x$, is 581 kcal/mole of cellulose, yielding a value of 0.39 for the ratio of net heat content to net heat of combustion. It may be seen from Fig. 15 that, except for a single point at high $A\sqrt{h}$, from 15 to 50 percent of the total lower heating value (3820 cal/g for complete combustion) of cellulose appears in the gaseous products. For a ventilation-limited enclosure, therefore, the major portion of the generated heat is transferred by radiation from the flames and glowing fuel. For a laboratory crib fire burning in the open, an overall heat balance showed that convective heat accounts for over 60 percent and radiative heat approximately 15 to 20 percent of the total heat evolved [17]

5. Summary

Results are presented of experimental measurements of the mass rates of burning, temperatues and gas compositions in model enclosures of three sizes. Interest was confined to the fully-developed stages of fires in which a single (or multiple) ventilation opening limited the burning rate of a reproducible crib-type cellulose-base combustible load.

The burning rate was found to be generally proportional to $A\sqrt{h}$ (A = area, h = height of window opening), but a characteristic transition region was found for each enclosure which resulted in a shift in the data line. The transition region is associated with a characteristic change in the position of flaming from predominantly within the crib to regions of more ready access of oxygen accompanied by a change in the fraction of the window opening used as inlet and exhaust ports. Burning rate data from the three sizes of enclosures were correlated in terms of the ventilation parameter $A\sqrt{h}$ and the exposed surface area of the crib, A_s. Despite a definite pattern of differences between the scales, a general concordance was found to exist. The maximum burning rate was found to be 7×10^{-4} g/sec per cm^2 of crib surface area for all scale sizes, and the location of the transition region corresponded to a value for $A\sqrt{h}/A_s$ of approximately 0.1 $cm^{1/2}$.

For each enclosure, the average temperature measured by thermocouples increased with $A\sqrt{h}/A_s$, but tended to level out for window openings greater than that at the transition region. There was a slight upward shift in temperature from the smallest to the largest size enclosure.

Continuous exhaust gas composition measurements were made by means of a sampling tube placed at the top front of the burning crib, using infrared absorption analyzers for CO and CO_2 and a magnetic susceptibility analyzer for O_2. At this sampling position, the CO percentage increased with $A\sqrt{h}$ for the two largest enclosures. The O_2 concentration decreased with $A\sqrt{h}$ and remained at or below 1 percent for window openings for which active flaming was observed, while the CO_2 concentration increased and remained above 16 to 18 percent.

Attempts were made to employ flow visualization techniques to measure the position of the neutral zone and the velocity profile across the window opening. The feasibility of simultaneous photographic recording of the neutral zone (from optical distortion of a background grid) and the velocity pattern of the hot exiting gases (from interrupted streak photography of low density particles) was examined but could not be perfected soon enough to be used throughout this test series.

Analysis of the combustion reaction in terms of the exhaust products was made. The measured CO/CO_2 ratios were found to increase slightly with the measured temperature at the probe inlet, and comparisons were made with temperature-equilibrium compositions of simple carbon combustion reactions.

The overall process involved in enclosure fires appears to be a combined gravity-controlled fluid dynamic regime and a radiation-controlled thermal regime. Although the similarity conditions are generally incompatible, partial modeling appears to be feasible if heat conduction through the boundary walls is the same in model and prototype. For a gravity- (buoyancy-) controlled regime, the dimensionless Froude group is the criterion for similarity, and, from the limited agreement found among the data for two enclosures, this group appears to include the essential parameters in the scaling of burning rates of fires in geometrically similar enclosures.

The heat content of the sampled product gases was calculated and its fraction of the total lower heat of combustion of cellulose was found to vary with A/h. It may be concluded that for a ventilation-limited enclosure, the major portion of the generated heat is transferred by radiation from the flames and glowing fuel.

6. Acknowledgments

The data summarized in this report were assembled through the combined efforts of permanent members of the Fire Research Section and a succession of college students serving 3-or 6-month training periods. It is a pleasure to acknowledge the determined efforts of the following student trainees: M. Heinemann, R. Kahn, J. Klein, D. Newman, P. Rauen, J. Sharlet, W. Snively, J. Stokley and G. Van Arsdale.

USCOMM-NBS-DC

7. References

[1] D. Gross, "Preliminary Results of Experimental Fires in Enclosures" NBS Tech. Report No. 7327, Aug 1961.

[2] P. H. Thomas, "Studies of Fires in Buildings Using Models," Research 13, pp. 69-77, 87-93, 1960.

[3] P. H. Thomas and A. J. M. Heselden, "Behavior of Fully Developed Fire in an Enclosure," Combustion and Flame, 6, pp. 133-5, 1962.

[4] D. Hird and C. F. Fischl, "Fire Hazard of Internal Linings" Department of Scientific and Industrial Research and Fire Offices' Committee, Special Report No. 22, H.M.S.O., London, 1954.

[5] K. Kawagoe, "Fire Behavior in Rooms," Building Research Institute Report No. 27, Ministry of Construction, Tokyo, Japan, 1958.

[6] H. D. Bruce, "Experimentsl Dwelling-Room Fires," Report No. D1941, Forest Products Laboratory, USDA, June 1953.

[7] D. Gross, "Experiments on the Burning of Cross Piles of Wood," NBS J. Research 66C, pp. 99-105, 1962.

[8] W. M. Rohsenow, "A Graphical Determination of Unshielded-Thermocouple Thermal Correction," Trans. ASME, 68, pp. 195-8, 1946.

[9] G. D. Van Arsdale, "An Investigation of the Fire-Induced Flow Regime at the Single Ventilation Opening in a Model Room Enclosure," NBS Tech. Report No. 7358, Oct 1961.

[10] R. T. Haslam and R. P. Russell, "Fuels and Their Combustion,"McGraw-Hill Book Co., New York, N. Y., 1926.

[11] F. L. Browne, "Theories of the Combustion of Wood and Its Control-A Survey of the Literature," Report No. 2136, Forest Products Laboratory, USDA, Dec 1958.

[12] D. D. Wagman, et al., "Heats, Free Energies and Equilibrium Constants of Some Reactions Involving O_2, H_2, H_2O, C, CO, CO_2 and CH_4. NBS J. of Research 34, pp. 143-161 (RP 1634) Feb 1945.

[13] C. Halpern, and F. W. Ruegg, "A Study of Sampling of Flame Gases," NBS J. Research 60, pp. 29-37, 1958.

[14] J. E. Emswiler, "The Neutral Zone in Ventilation," Trans. ASHVE, 32, pp. 59-74, 1926.

[15] W. G. Brown, and K. R. Solvason, "Natural Convection Theory to Rectangular Openings in Partitions, Part I. Vertical Partitions," Intern'l J. of Heat and Mass Transfer, 5, pp. 859-868, 1962.

[16] F. D. Rossini, et al., "Selected Values of Properties of Hydrocarbons," NBS Circular 461, 1947.

[17] W. L. Fons, et al., "Project Fire Model," Summary Progress Report I (1960) and II (1962), Forest Service, USDA.

Table 1. Construction Details of Model Enclosures

Model	Size-Internal Dimensions				Wall Construction						Method of Weighing
					Outer Skin		Insulation				
	Width	Height	Length	Vol.	Mat'l	Thickness	Mat'l	Thickness	Density	Thermal Conductivity	
	cm	cm	cm	cm^3		cm		cm	g/cm^3	cal/sec cm °C	
I	16.2	16.7	33.7	9.1×10^3	Steel	.16	Calcium Silicate	0.64	0.40	.00016	Entire box supported directly on platform balance scale
II	46.7	44.7	98.0	2.2×10^5	Steel	.16	Asbestos Millboard	1.27	0.86	.00029	Entire box supported directly on platform balance scale
III	146	145	305	6.5×10^6	Steel	.16	Lean mix perlite gypsum plaster with foaming agent	2.5	0.43	.00028	Crib only supported on balance by means of platform whose legs passed through floor of enclosure

Table 2. Summary of Test Results

Table 2. Summary of Test Results

Test No.	A	h	$A\sqrt{h}$	$\frac{A\sqrt{h}}{As}$	r	$\frac{r}{As}$	T	Gas Composition, Dry O_2	CO	CO_2	$\frac{CO}{CO_2}$	x	f	n	G	N_{ER}
	cm^2	cm	$cm^{5/2}$	$cm^{1/2}$	g/sec	10^3g/sec cm^2	°C	%	%	%					cm^3/g	
SCALE I				Horizontal Window												
24	27.5	1.70	35.9	.0377	.0582	.0609	500									
23	41.3	2.55	66.4	.0697	.0833	.0872	275									
22	55.1	3.40	102	.107	.101	.106	400									
21	63.3	3.91	125	.131	.100	.105	420									
18	68.9	4.25	142	.149	.0945	.0997	405									
19	74.4	4.59	159	.167	.0953	.0998	375									
20	79.9	4.93	177	.186	.123	.129	450									
11	82.6	5.10	187	.196	.174	.183	445									
15	90.9	5.61	216	.227	.189	.198	475									
17	96.4	5.95	236	.248	.196	.207	425									
16	102	6.29	256	.269	.277	.291	500									
13	110	6.80	287	.302	.353	.371	420									
55	do	do	do	.173	.174	.105	535									
56	do	do	do	.211	.212	.156	525									
58	do	do	do	.232	.272	.219	-									
62	do	do	do	.259	.280	.252	550									
54	do	do	do	.301	.340	.357	475									
61	do	do	do	.775	.219	.592	-									
60	do	do	do	.600	.302	.631	425									
59	do	do	do	.591	.363	.750	470									
63	do	do	do	1.25	.234	1.02	655									
12	124	7.65	343	.360	.484	.508	475									
6	138	8.50	402	.422	.590	.620	545									
8	207	12.8	740	.777	.658	.691	540									
3	270	16.7	1100	1.22	.636	.667	645									
				Dual Horizontal Windows*												
48	7.3	0.45	44.3	.0466	.0953	.100	248									
49	17.0	1.05	103	.108	.0975	.102	410									
40	23.0	1.42	137	.144	.113	.118	-									
42	43.9	2.71	257	.270	.232	.243	450									
43	52.0	3.21	302	.316	.404	.423	525									
44	60.6	3.74	350	.366	.446	.468	550									
45	68.4	4.22	391	.409	.461	.484	525									
46	76.8	4.74	435	.456	.471	.495	560									
47	104	6.42	570	.598	.714	.748	525									
39	147	9.10	770	.809	.665	.697	550									
				Vertical Window												
31	14.2	16.7	58.0	.0609	.0688	.0724	230									
33	17.0	do	69.6	.0731	.0991	.104	300									
32	19.9	do	81.2	.0853	.132	.139	325									
30	22.7	do	92.9	.0975	.189	.198	320									
34	28.4	do	116	.122	.207	.217	400									
35	34.1	do	139	.146	.154	.162	485									
28	42.6	do	174	.183	.129	.135	575									
36	48.3	do	197	.207	.152	.160	525									
29	56.8	do	232	.244	.189	.198	655									
37	65.3	do	266	.279	.257	.271	550									
27	71.0	do	290	.304	.522	.548	525									
26	99.4	do	406	.426	.603	.632	600									
38	114	do	464	.487	.636	.667	-									
25	142	do	596	.625	.683	.717	650									

* "Effective" $A\sqrt{h}$ values are listed.

SCALE II				Horizontal Window												
18A	109	2.35	167	.0143	.0923	.00773	128									
6	121	2.59	195	.0168	.176	.0151	150	12	3.2	6.0	0.53	.65	7.8	2.1	14,200	1.63
17A	174	3.76	338	.0290	.505	.0438	215									
16A	218	4.70	473	.0406	.765	.0653	270									
7A	260	5.60	616	.0529	1.02	.0876	305									
6A	329	7.10	876	.0752	1.71	.147	310									
10A	385	8.30	1110	.0953	1.84	.158	485									
7	430	9.2	1300	.117	2.04	.175	600	1.0	7.0	18.5	0.38	.73	.24	0.90	13,900	1.02
3	471	10.1	1500	.129	2.22	.191	-	0.1	6.5	20.0	0.32	.75	.02	0.88	-	-
23A	545	11.8	1870	.161	2.35	.202	645									
9B	654	14.1	2450	.839	2.42	.829	635									
7B	do	do	do	.352	3.03	.436	-									
8B	do	do	do	.280	3.33	.380	670									
2B	do	do	do	.210	3.62	.311	-									
12B	do	do	do	.176	3.34	.240	665									
11B	do	do	do	.150	2.75	.169	635									
10B	do	do	do	.104	2.64	.112	550									
1A	do	do	do	.211	3.83	.329	610									
4	747	16.0	3000	.258	5.25	.451	675	1.5	10	19	9.53	.66	.31	0.88	14,900	1.29
14A	835	18.0	3540	.304	6.10	.524	540									
13A	1020	22.0	4790	.411	7.76	.607	605									
9	1320	28.2	7000	.601	8.10	.696	750	0.1	13.7	19	0.72	.58	.02	0.78	14,700	0.49
12A	1640	35.2	9720	.835	9.38	.806	550									
31A	2180	46.7	14900	1.28	9.15	.786	-									
				Vertical Window												
33	48	47.7	330	.0283	.369	.0314	220	7.8	4.3	9.9	0.43	.70	3.3	1.4	11,500	1.26
37	72	do	500	.0430	.515	.0443	200									
31	100	do	700	.0601	1.29	.111	350	1.2	6.3	18	0.35	.74	0.3	0.92	10,100	1.31
30	114	do	800	.0687	1.41	.121	355	0.5	6.3	19	0.33	.75	.12	0.90	9,940	1.14
29	144	do	1000	.0859	2.26	.194	355	0.8	7.0	18.5	0.38	.73	.19	0.90	9,940	1.88
34	188	do	1300	.117	2.67	.229	375	0.5	7.2	19.2	0.38	.73	.11	0.88	10,100	1.51
51	204	do	1400	.120	2.73	.235	400	0.2	7.7	18.7	0.41	.71	.05	0.86	10,300	1.33
15	217	do	1500	.129	2.45	.210	480	-	8.4	19.7	0.43	.70	-	-	-	-
14	260	do	1800	.155	2.50	.215	520	0.8	7.3	19.5	0.37	.73	.18	0.90	12,600	0.76
25	305	do	2100	.180	2.89	.248	565	0.2	9.5	>20	<0.48	.68	.04	0.85	12,800	.71
46	362	do	2500	.215	2.84	.244	575	<0.1	11.2	>19.7	<0.57	.64	.02	0.82	12,600	.46
44	505	do	3500	.301	3.45	.296	645	0	9.5	19.5	0.49	.67	.00	0.84	13,900	.37
28	578	do	4000	.344	4.48	.383	645	0.5	>11.5	18.8	>0.61	.62	.10	0.83	13,800	.48
45	658	do	4550	.391	4.92	.423	660	0.2	>12.3	19.4	>0.63	.61	.04	0.81	13,800	.43
32	725	do	5000	.430	5.57	.478	640	0.2	>13.9	18.7	>0.74	.57	.04	0.79	13,300	.44
48	797	do	5500	.472	6.13	.527	680	<0.1	>11.7	>20	>0.58	.63	.02	0.82	14,200	.47
47	878	do	6000	.515	6.71	.576	675	<0.1	>14.0	19.2	>0.73	.58	.02	0.79	13,800	.45
38	940	do	6500	.558	6.68	.574	655	0.5	>14.0	19.3	>0.73	.58	.09	0.80	13,700	.39
49	1080	do	7500	.644	6.96	.598	675	0.3	>13.0	19	>0.68	.59	.06	0.80	13,900	.31
43	1120	do	7750	.666	7.43	.638	665	0.5	>14	19.5	>0.72	.58	.09	0.80	13,800	.33
50	1740	do	12000	1.03	8.71	.748	685	0.5	>12	17.7	>0.68	.60	.10	0.82	14,200	.20
36	2230	do	17400	1.49	8.48	.728	750	0.5	>14	18.6	>0.75	.57	.09	0.80	15,100	.09
SCALE III				Horizontal Window												
6	1130	7.80	3180	.0335	4.01	.0422	232	10.3	3.7	8.3	.45	.69	5.1	1.7	14,700	1.89
10	1340	9.24	4080	.0431	9.75	.103	410	7.9	5.6	10.1	.55	.65	3.0	1.1	13,000	1.08
7	1510	10.4	4900	.0517	11.6	.122	550	0.3	5.9	18.0	.33	.75	0.08	0.89	13,000	2.22
11	2190	15.1	8560	.0815	22.8	.216	-	0.1	5.3	19.3	.28	.79	0.24	0.92	-	-
8	2600	17.8	11000	.105	13.9	.132	668	3.9	3.1	14.7	.21	.83	1.3	1.1	17,900	0.98
12	2970	20.5	13500	.117	20.6	.178	785	2.9	3.0	15.4	.20	.84	0.96	1.3	23,200	2.03
9	3910	27.0	20500	.162	40.4	.319	874	0.9	5.7	16.8	.34	.75	0.24	0.89	18,000	1.82
13	6020	41.6	29200	.280	60.0	.428	1020	0.1	8.6	16.6	.52	.65	0.02	0.94	21,300	1.31
				Vertical Window												
14	320	145	3850	.0406	10.3	.108	350	8.3	5.5	10.5	.52	.65	3.1	1.1	11,800	1.80
1	565	do	6900	.0412	13.7	.0818	550	3.7	3.8	15.1	.25	.80	1.2	1.1	15,700	2.28
15	736	do	8850	.102	13.8	.159	668	0.1	2.3	18.0	.13	.89	0.03	0.95	15,500	1.12
17	1660	do	19700	.148	31.0	.233	745	1.0	8.0	18.5	.43	.70	0.23	0.89	16,000	1.08
18	1660	do	do	.0827	29.5	.124	749	1.0	6.9	17.7	.39	.72	0.24	0.90	16,400	1.03
21	1660	do	20000	.152	19.9	.151	710	-	-	-	-	-	-	-	-	-
2	2610	do	31900	.336	46.7	.514	875	-	-	-	-	-	-	-	-	-
3	4130	do	50400	.302	64.0	.383	920	0.0	13.5	17.1	.79	.56	0.0	0.78	17,500	0.63
4	8180	do	100,000	1.056	50.0	.527	850								-	-
16	8180	do	do	.598	103	.617	1039	0.8	8.8	16.4	.54	.65	0.20	0.86	20,200	0.52
19	8180	do	do	.487	161	.786	971	0.5	8.1	16.4	.49	.67	0.12	0.86	19,100	1.23
5	12260	do	150,000	.898	93.1	.556	950	5.5	2.2	13.7	.16	.86	2.1	1.3	26,900	.37
20	21200	do	256,000	1.095	122	.521	1090	11.8	0.3	7.5	.04	.96	9.1	2.5	53,300	.74

Table 3. Effect of Crib Construction on Rate of Burning
Scale II Enclosure
$A\sqrt{h} = 2500$ cm$^{5/2}$

Test No.	Spacing (in stick widths)	Initial Crib Weight g	Mean Rate of Burning g/sec
62	1	2730	3.05
61	2	2730	2.98
60	3	2740	3.34
63	5	2780	4.43

Table 4. Gas Composition Measurements Using Cooled and Uncooled Probes.

Gas	Composition, mole percent			
	Mass Spectrometer		Continuous Infrared Analyzer	
	Cooled Probe	Uncooled Probe	Cooled Probe	Uncooled Probe
CO	1.2	4.1	1.9	5.4
CO_2	1.5	7.4	4.1	15.0
O_2	20.4	12.8		
N_2	68.2	74.7		
Ar	1.0	0.9		
H_2O	7.8	---		
CO/CO_2	0.8	0.55	0.46	0.36

T = 580°C

Table 5. Sample Calculation of the Heat Content of the Measured Exhaust Gases

Scale III, Test 9, $A\sqrt{H} = 20,500\ cm^{5/2}$, T = 1147 °K, x = 0.75, f = 0.24

Component	Measured Mole Fraction dry	Mole Fraction wet	Heat Content of Component[a] at Temp. T kcal/mole of component	Heat Content of Component[a] at Temp. T kcal/mole of products	Heat Content of Component[a] at 25°C(298°K) kcal/mole of component	Heat Content of Component[a] at 25°C(298°K) kcal/mole of products
CO_2	.168	.142	12.16	1.73	2.24	0.32
CO	.057	.048	8.44	.40	2.07	0.10
O_2	.009	.007	8.73	.06	2.07	0.01
N_2(by difference)	.766	.646	8.37	5.41	2.07	1.34
H_2O	-	.157	10.07	1.58	2.36	0.37
				9.18		2.14

[a] From ref [167]

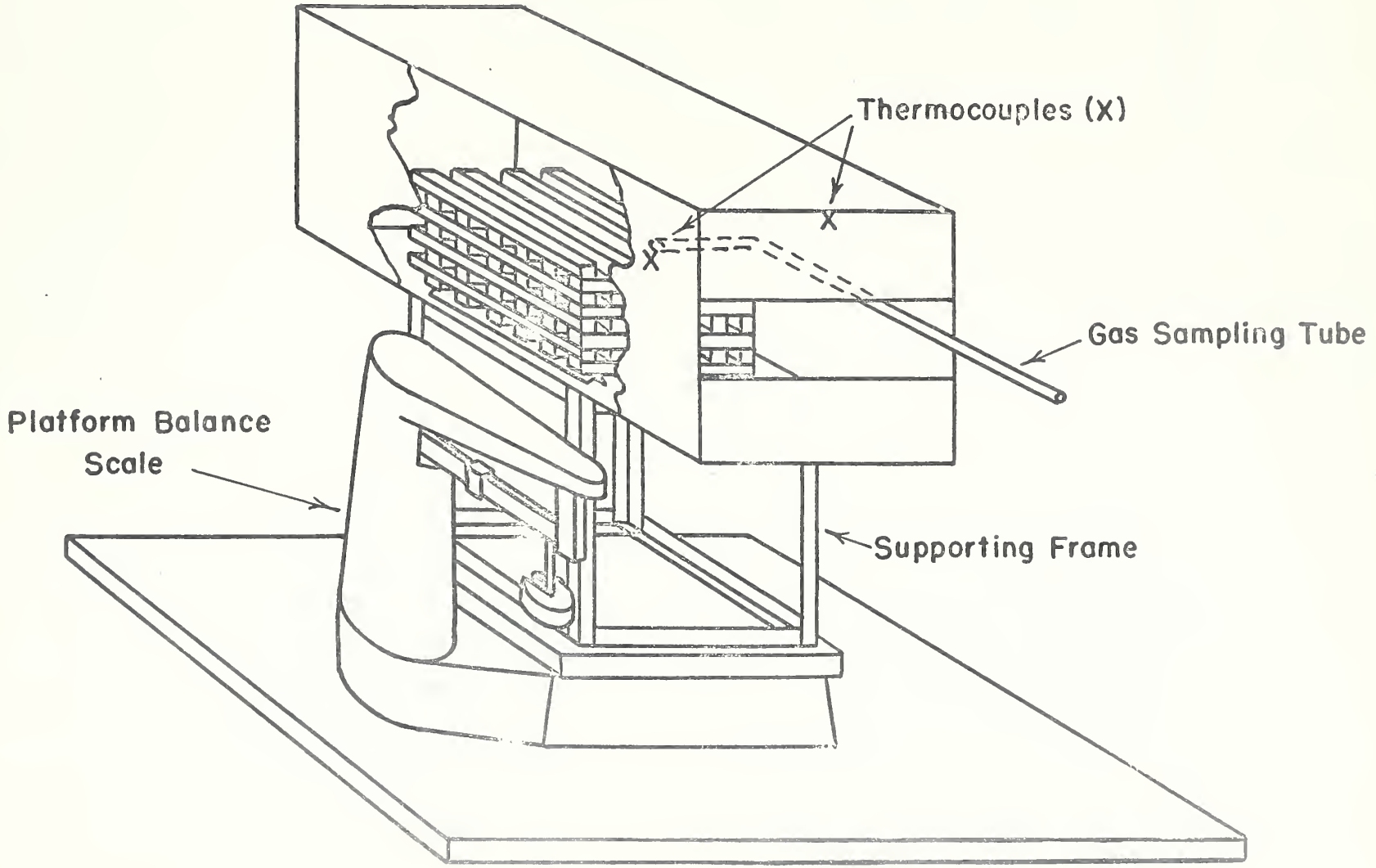

FIG. 1 - SCHEMATIC DIAGRAM OF EXPERIMENTAL APPARATUS

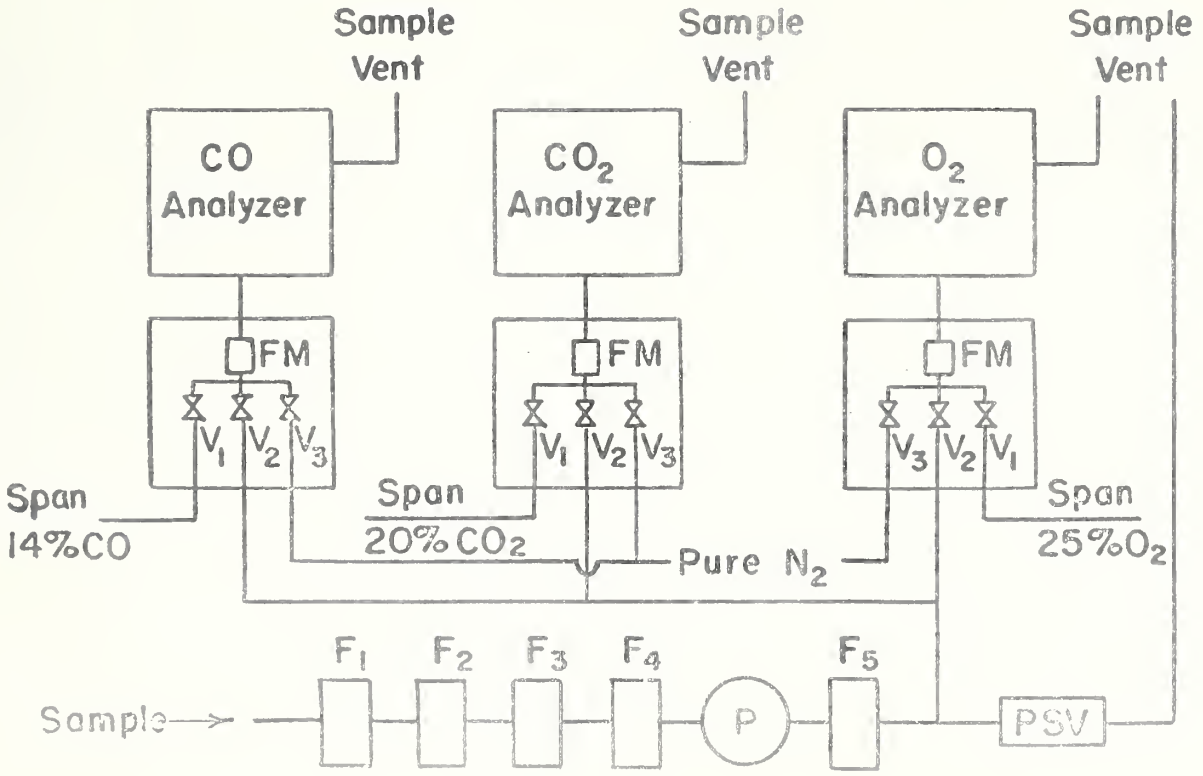

F_1 Tar and Resin Trap
F_2 Moisture Trap
F_3 F_4 F_5 Air Line Filters
P Pump
FM Flow Meter
PSV Relief-By-Pass Valve (1 PSIG)

FIG. 2 - SKETCH OF GAS SAMPLING ARRANGEMENT

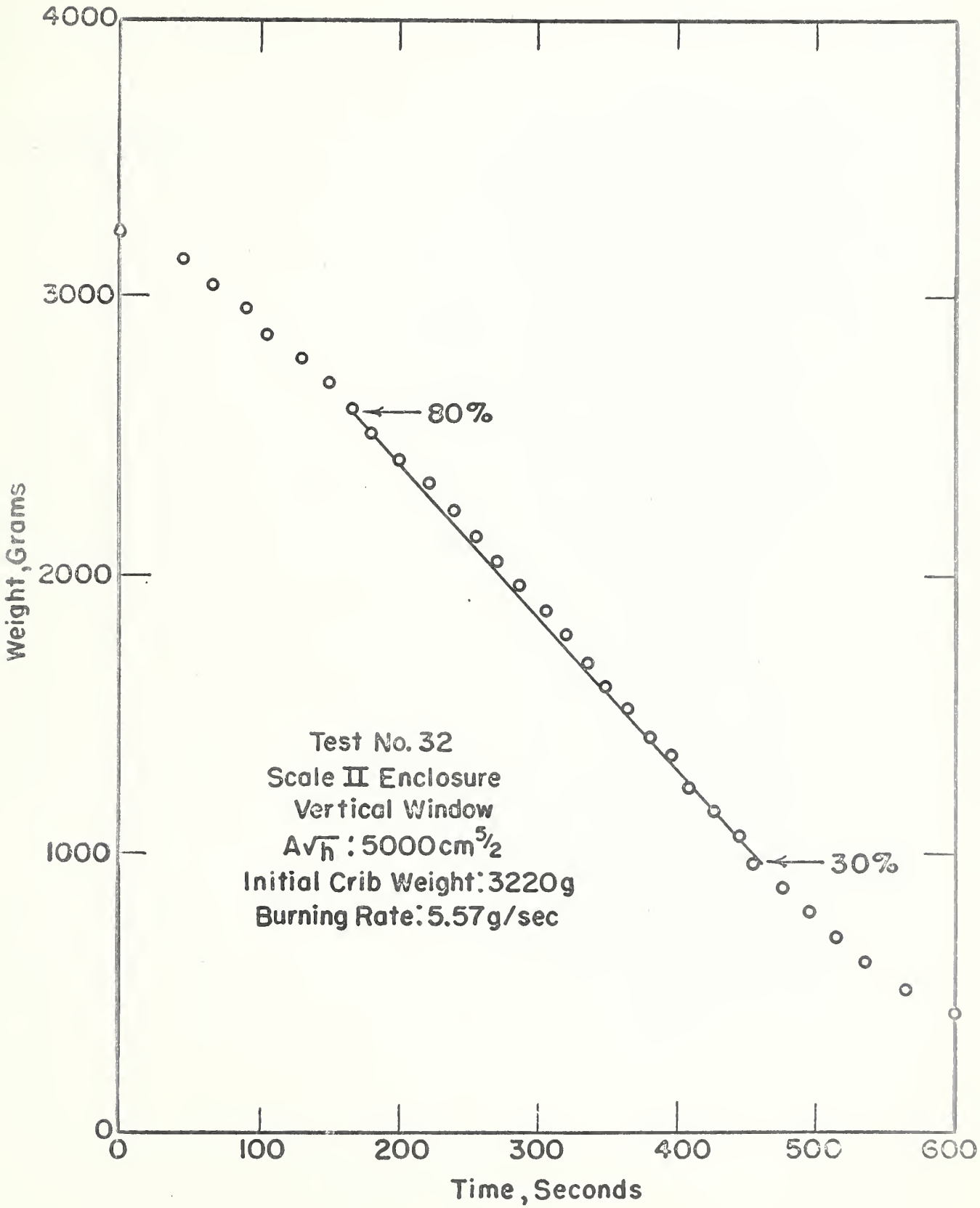

FIG. 3 - TYPICAL WEIGHT-TIME RECORD

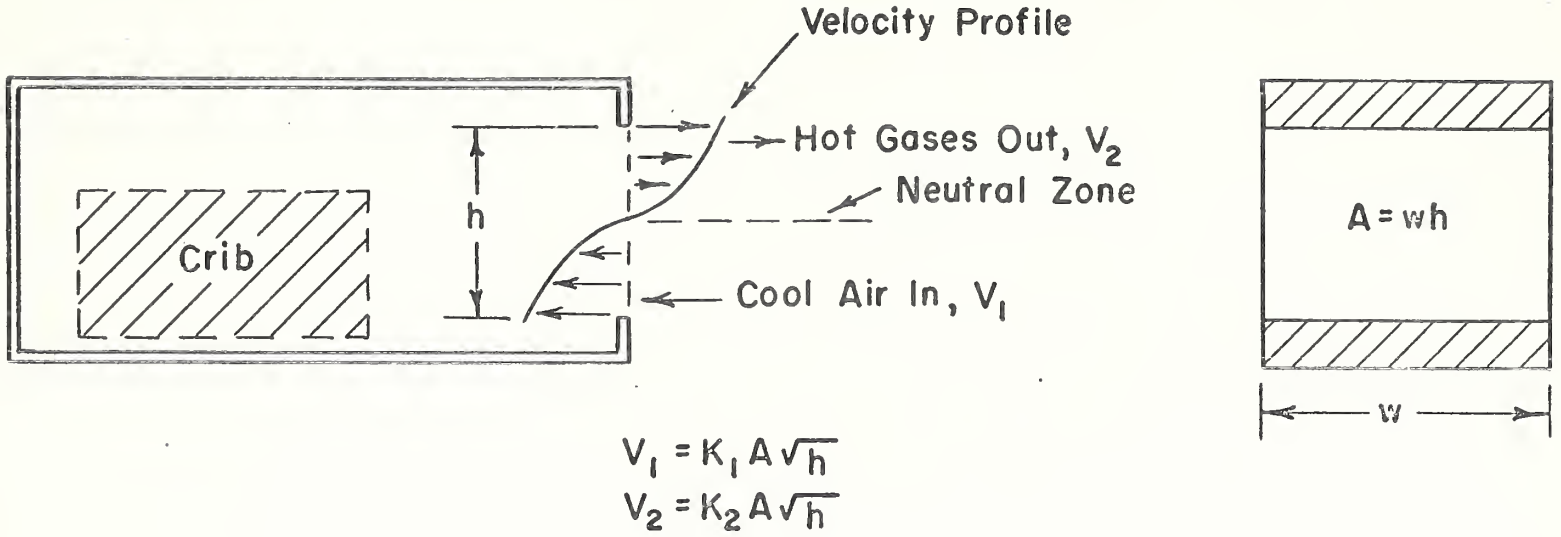

FIG.4 – IDEALIZED FLOW THROUGH WINDOW OPENING

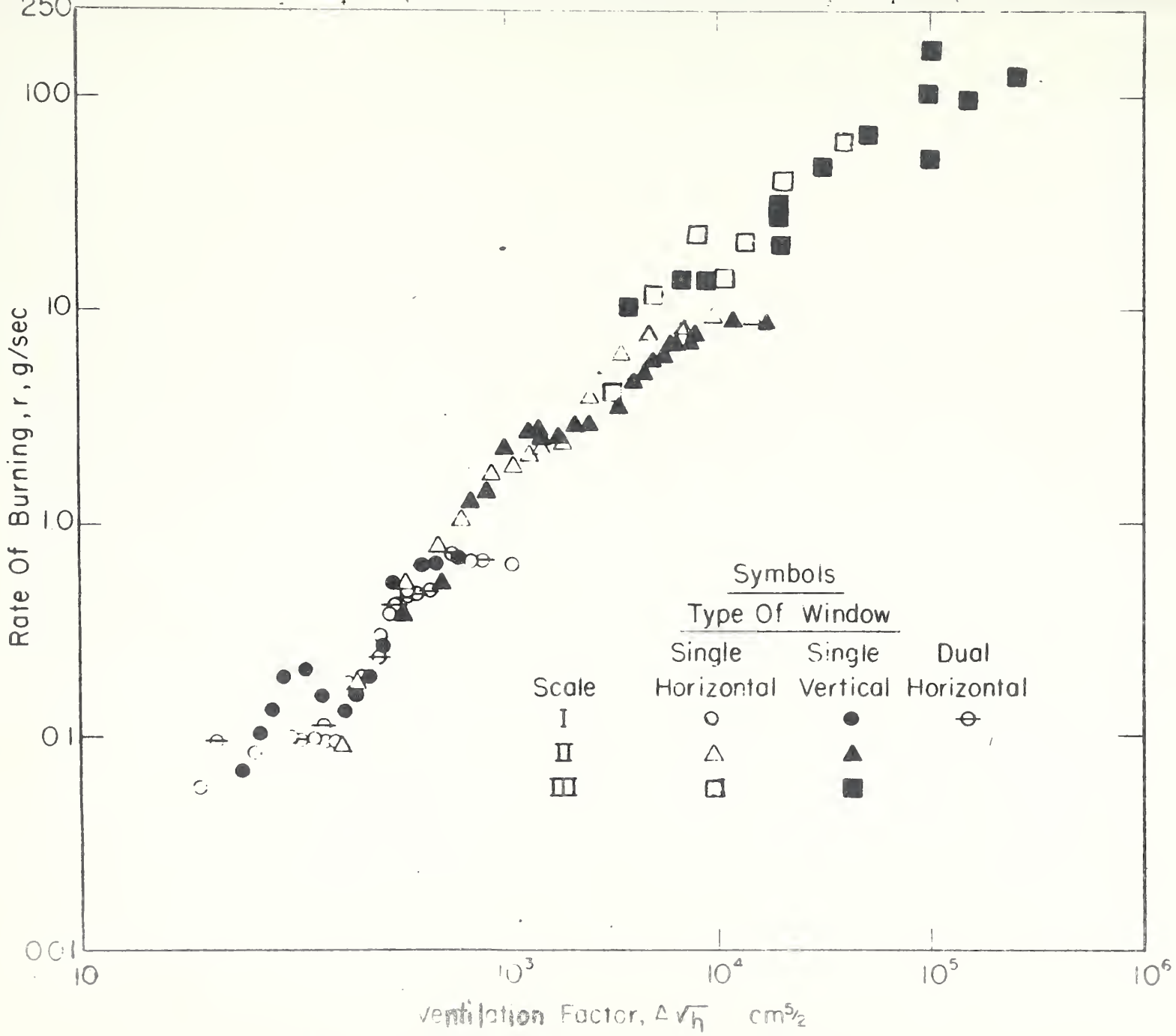

FIG. 5 - BURNING RATE AND VENTILATION FACTOR FOR THREE ENCLOSURES

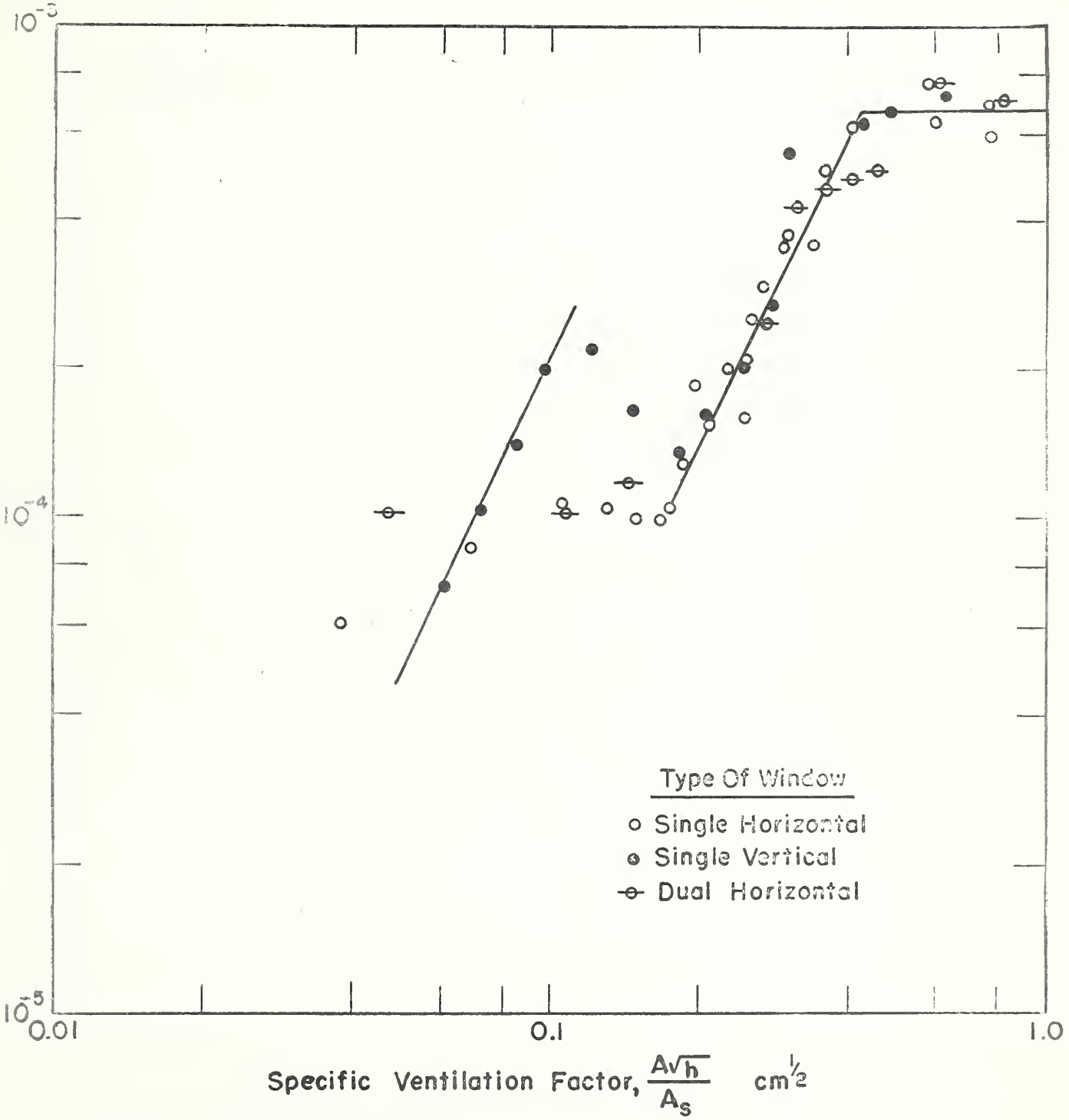

FIG.6A-SPECIFIC BURNING RATES AND VENTILATION FACTORS FOR SCALE I ENCLOSURE

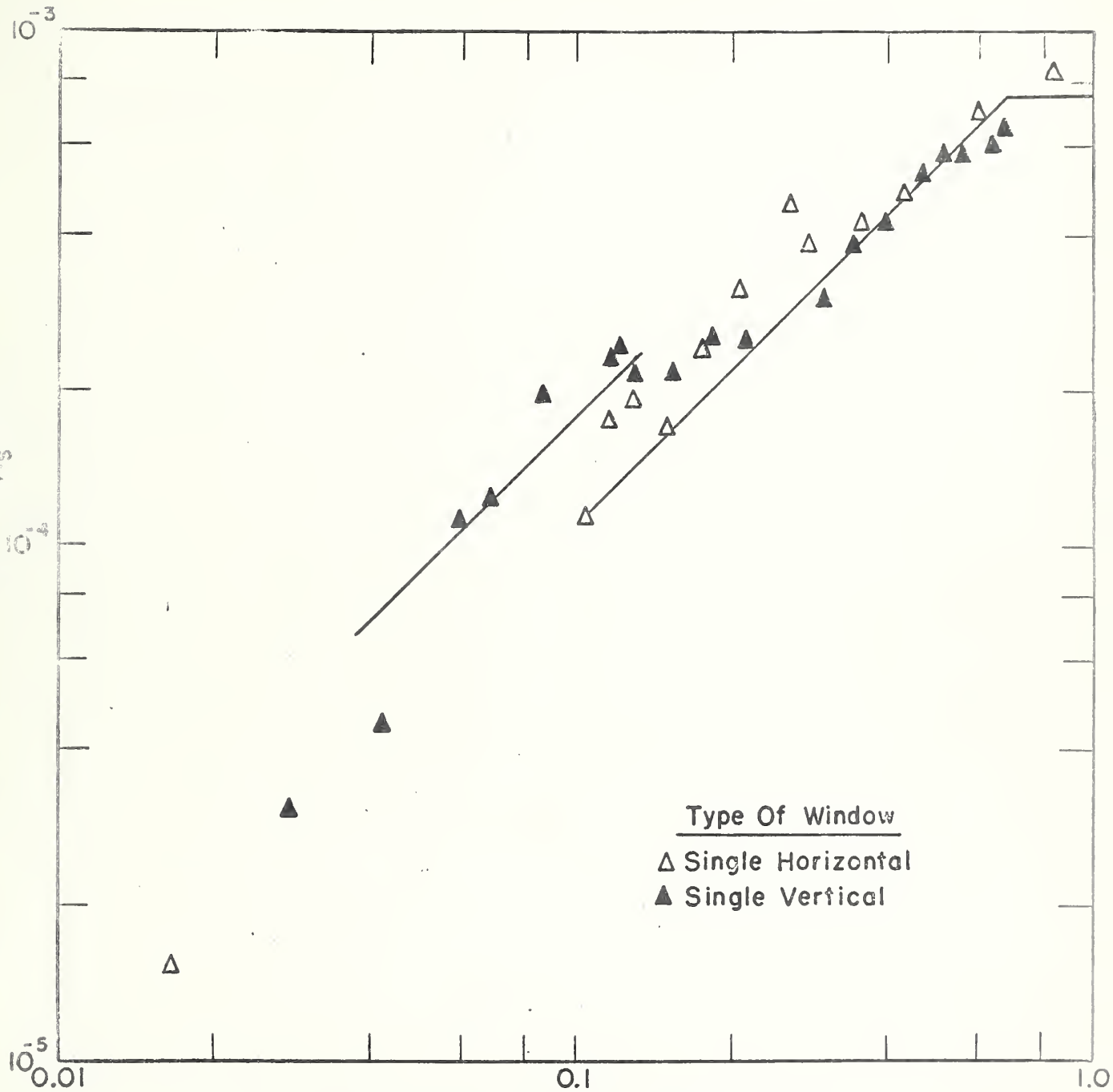

FIG. 6B - SPECIFIC BURNING RATES AND VENTILATION FACTORS FOR SCALE II ENCLOSURE

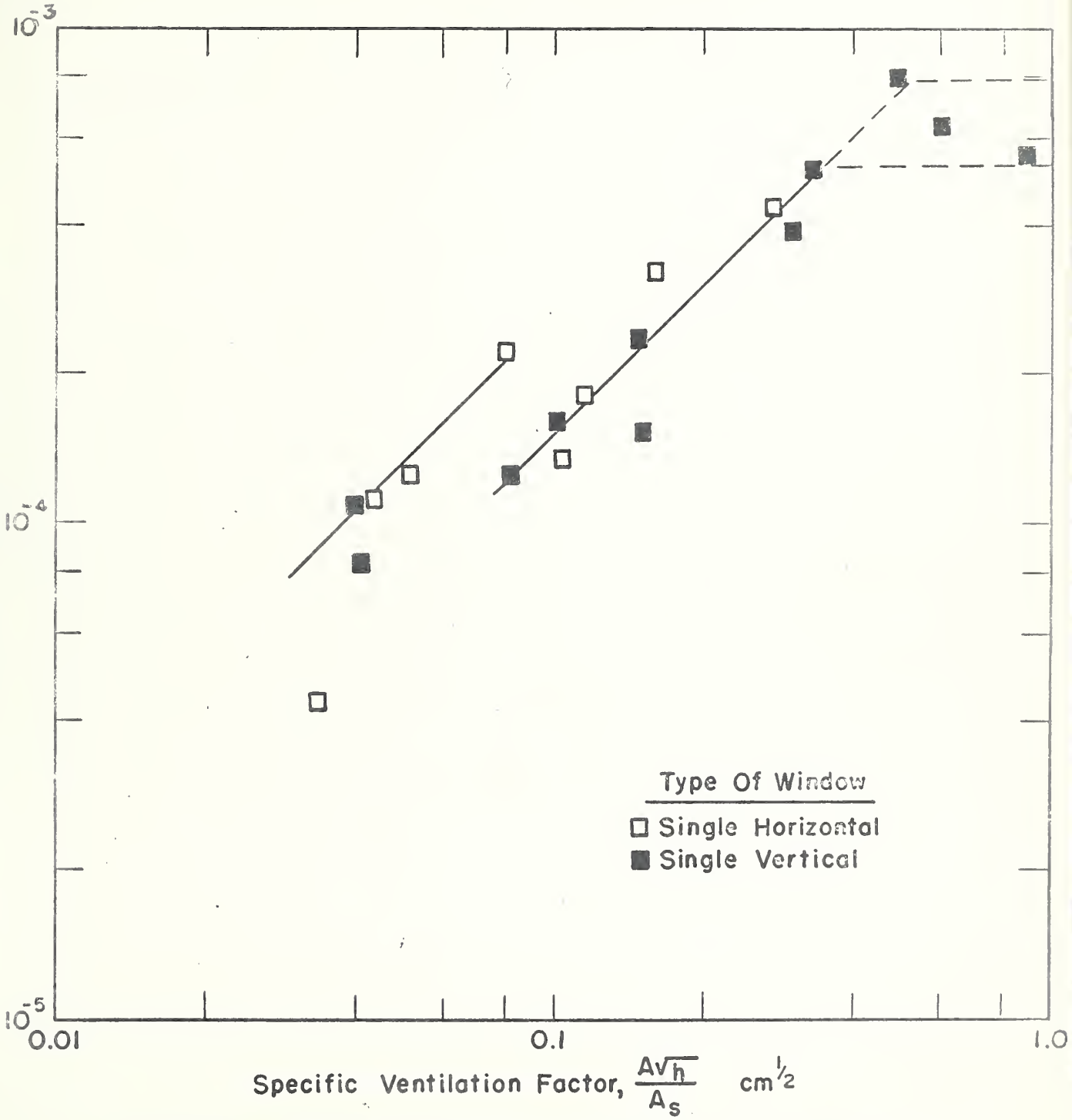

FIG.6C - SPECIFIC BURNING RATES AND VENTILATION FACTORS FOR SCALE III ENCLOSURE

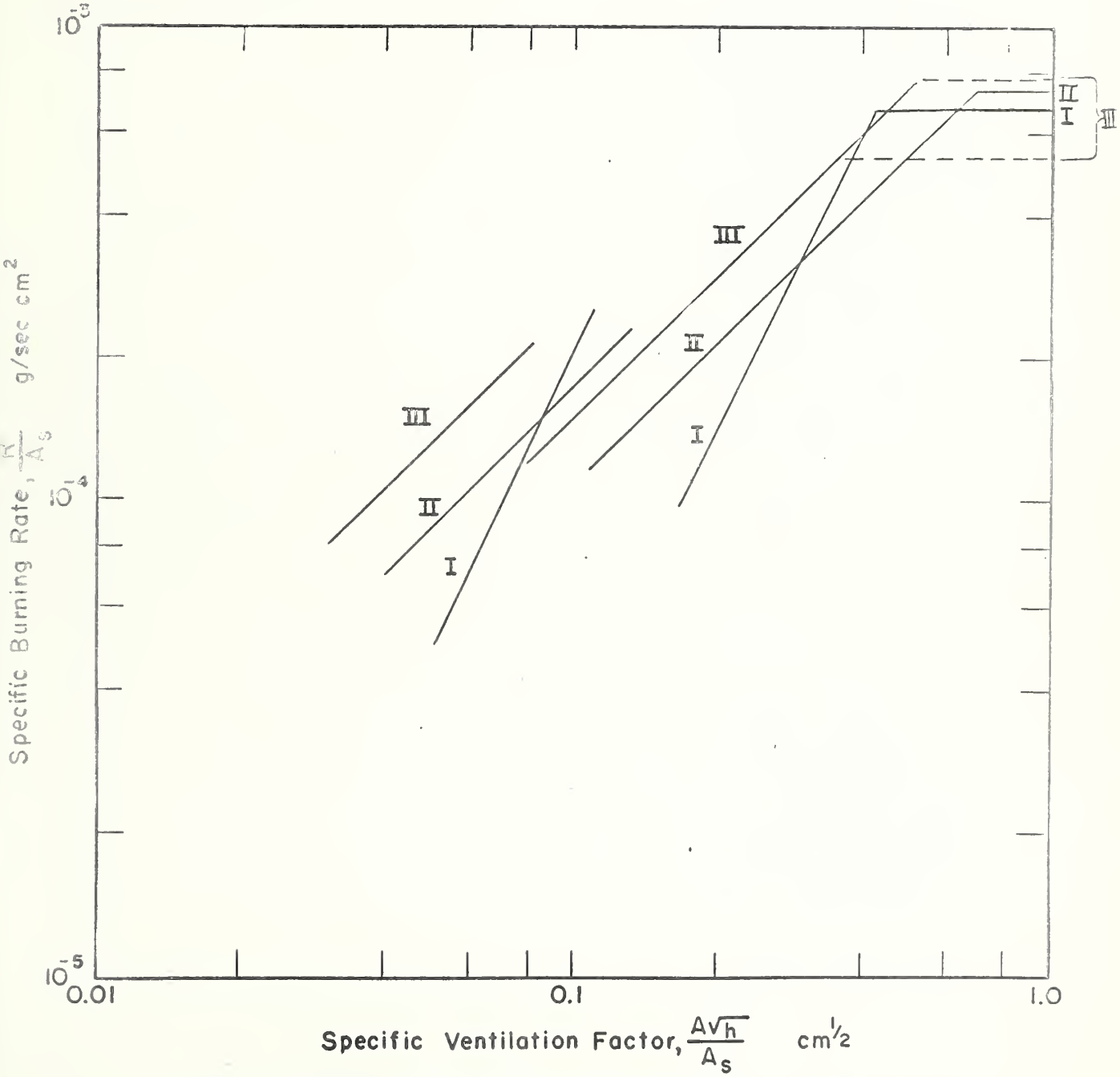

FIG.7–SPECIFIC BURNING RATES AND VENTILATION FACTORS FOR THREE ENCLOSURES, "BEST FIT" LINES

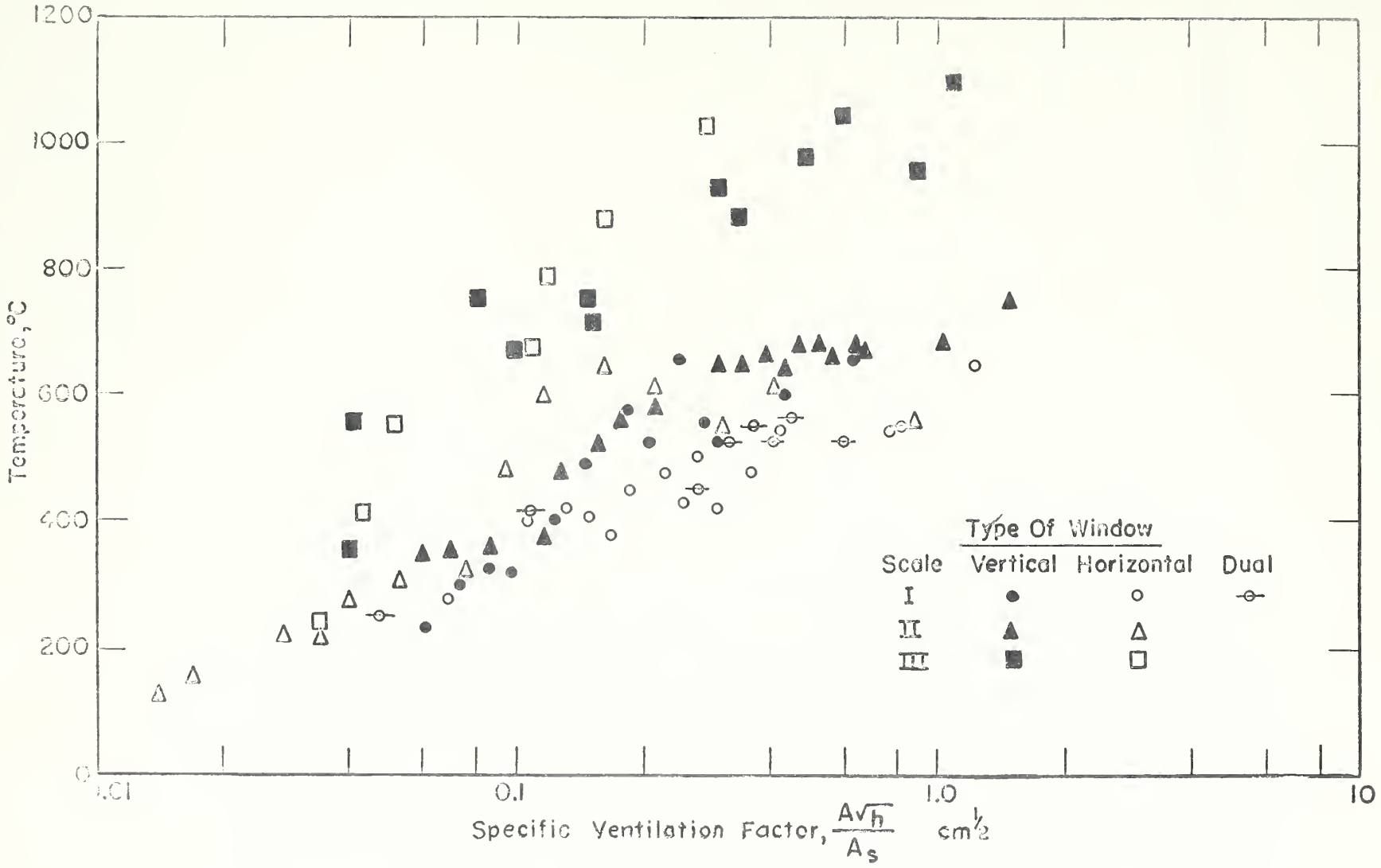

FIG.8 – TIME-AVERAGED TEMPERATURES FOR THREE ENCLOSURES

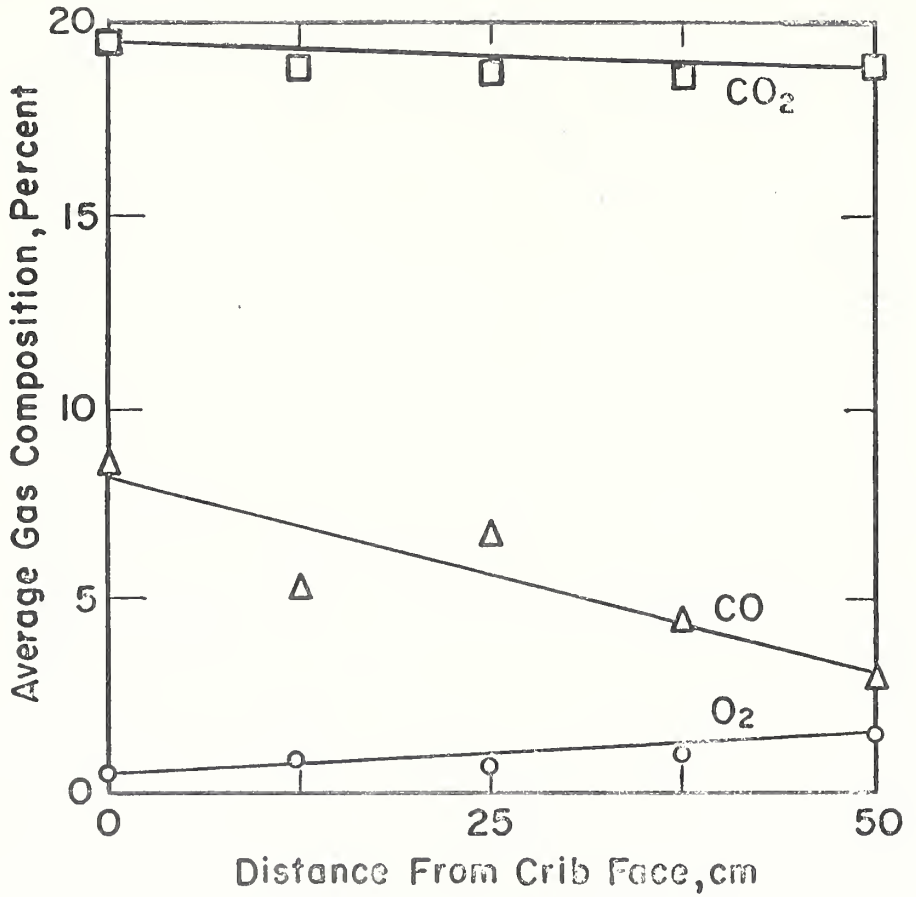

FIG.9-VARIATION IN TIME-AVERAGED GAS COMPOSITION WITH HORIZONTAL LOCATION OF SAMPLING PROBE SCALE II ENCLOSURE

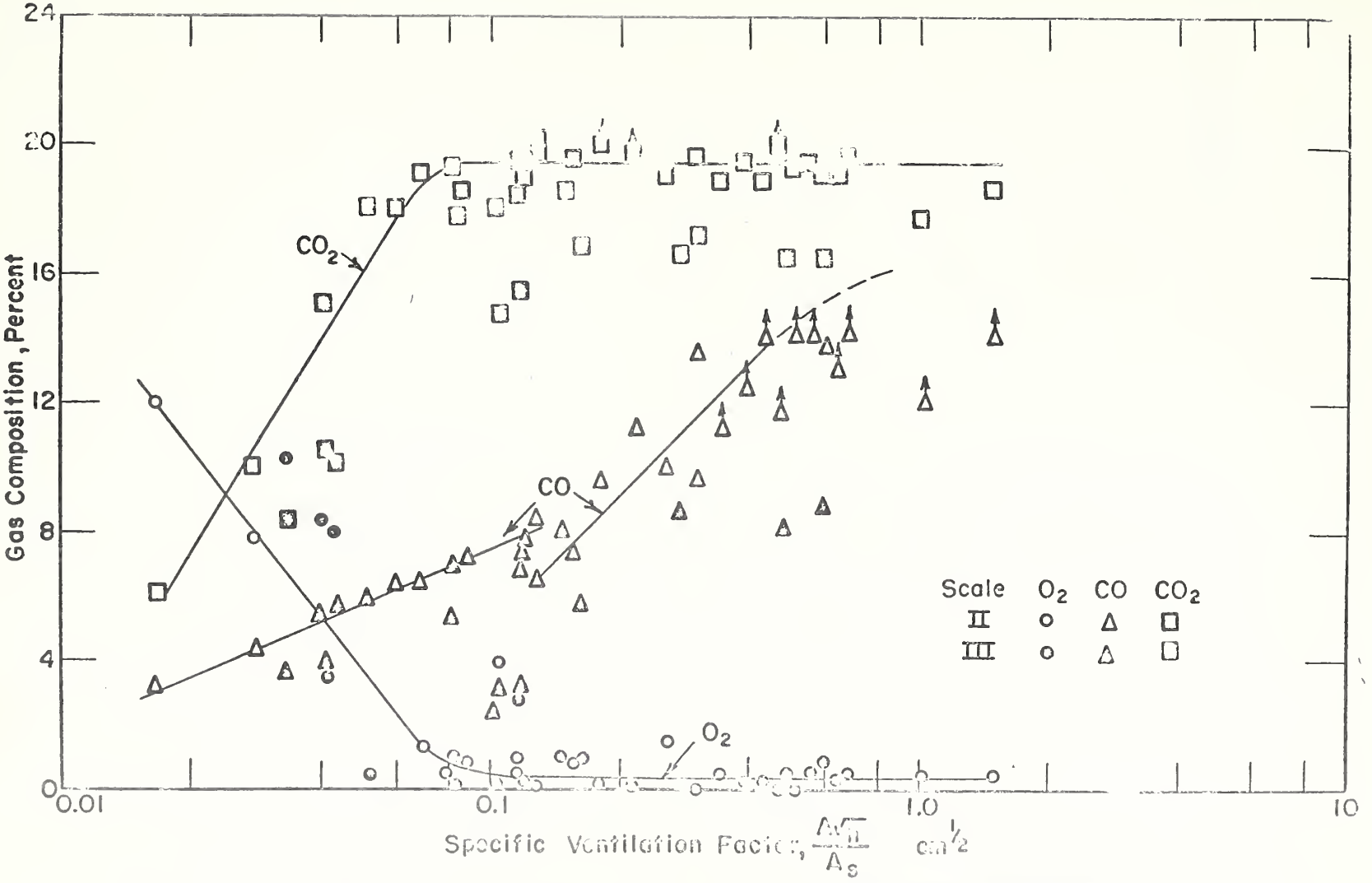

FIG. 10 – TIME-AVERAGED GAS COMPOSITIONS AND VENTILATION FACTORS

Lines Drawn Represent Estimated "Best Fit" Trend Lines For Data From Scale II Enclosure
↑ Higher Value Indicated For Readings Beyond Full-Scale

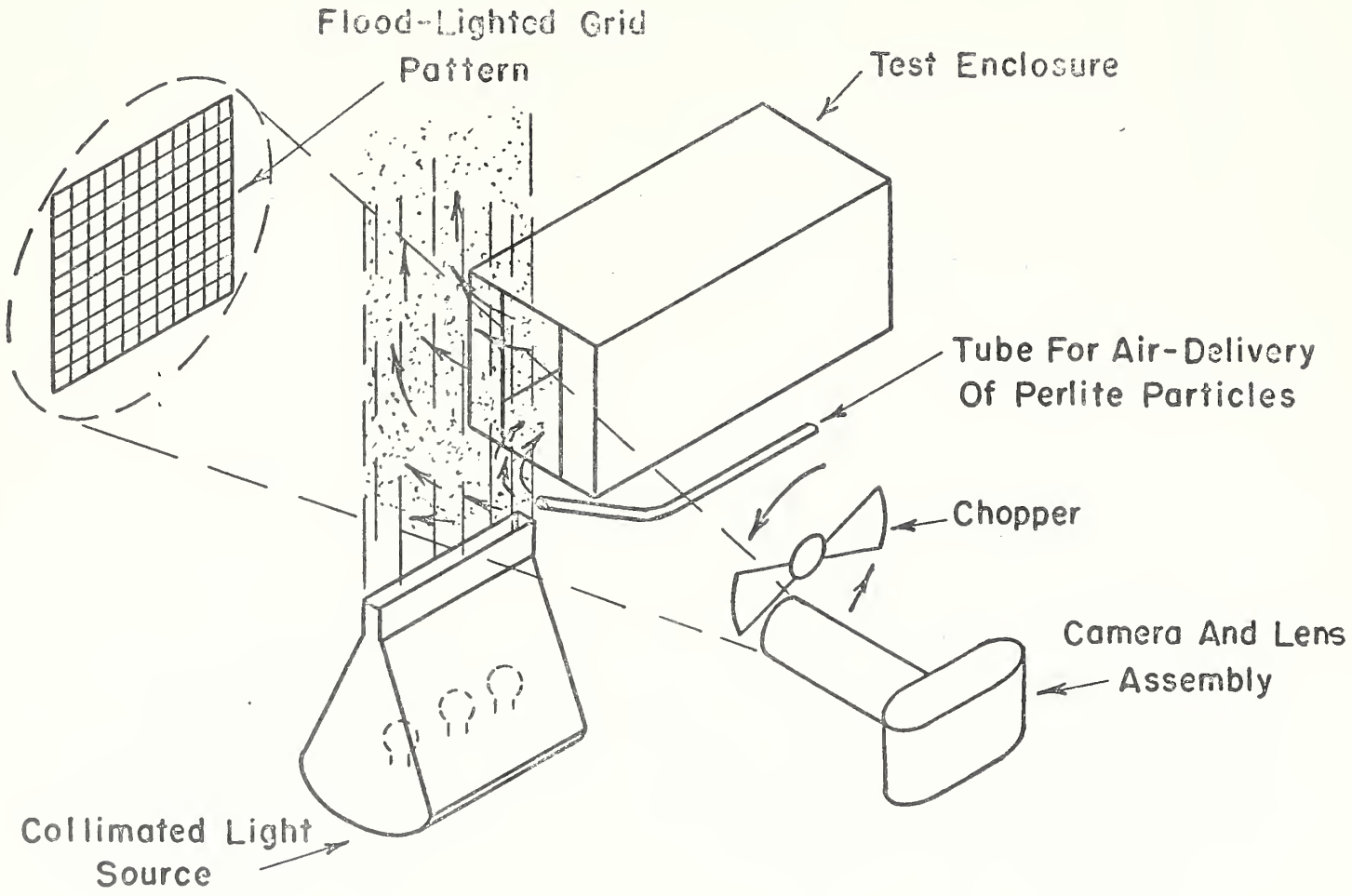

FIG. II – SCHEMATIC DIAGRAM OF APPARATUS FOR FLOW VISUALIZATION STUDIES

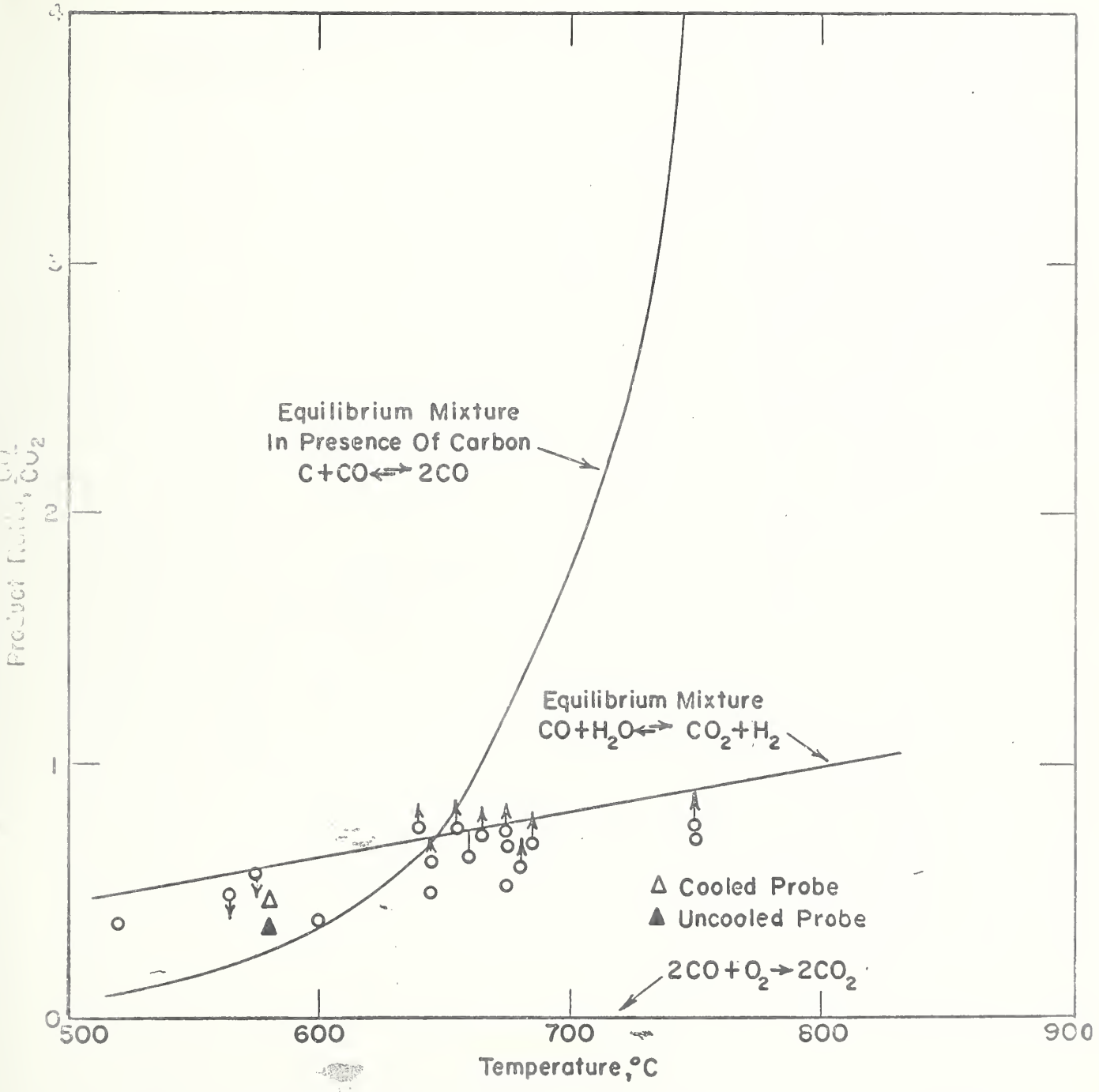

FIG.12 - TEMPERATURE - EQUILIBRIUM COMPOSITIONS FOR SIMPLE COMBUSTION REACTIONS, THEORETICAL AND EXPERIMENTAL

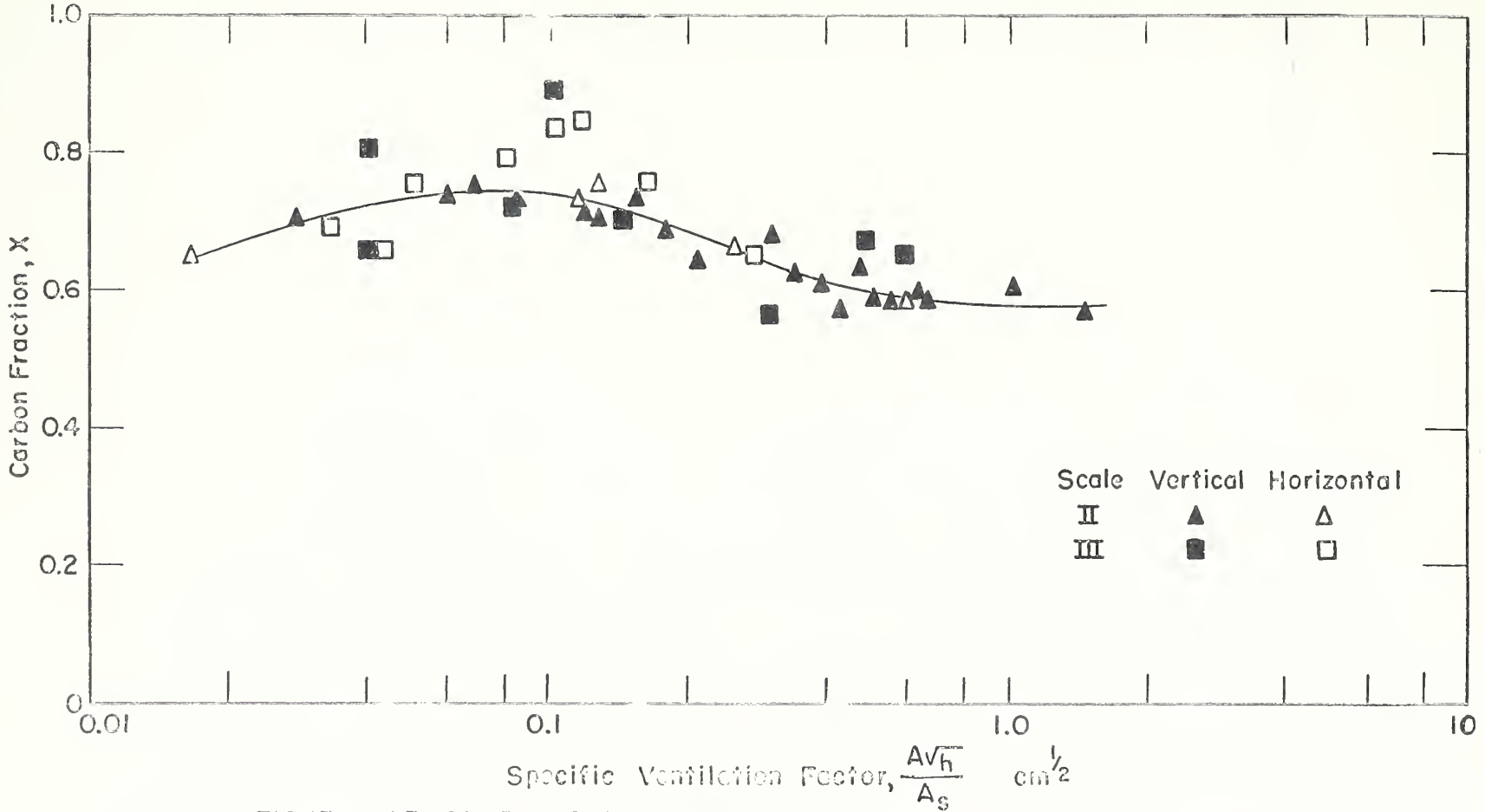

FIG. 13 - CARBON FRACTION APPEARING AS CO_2 FOR TWO ENCLOSURES

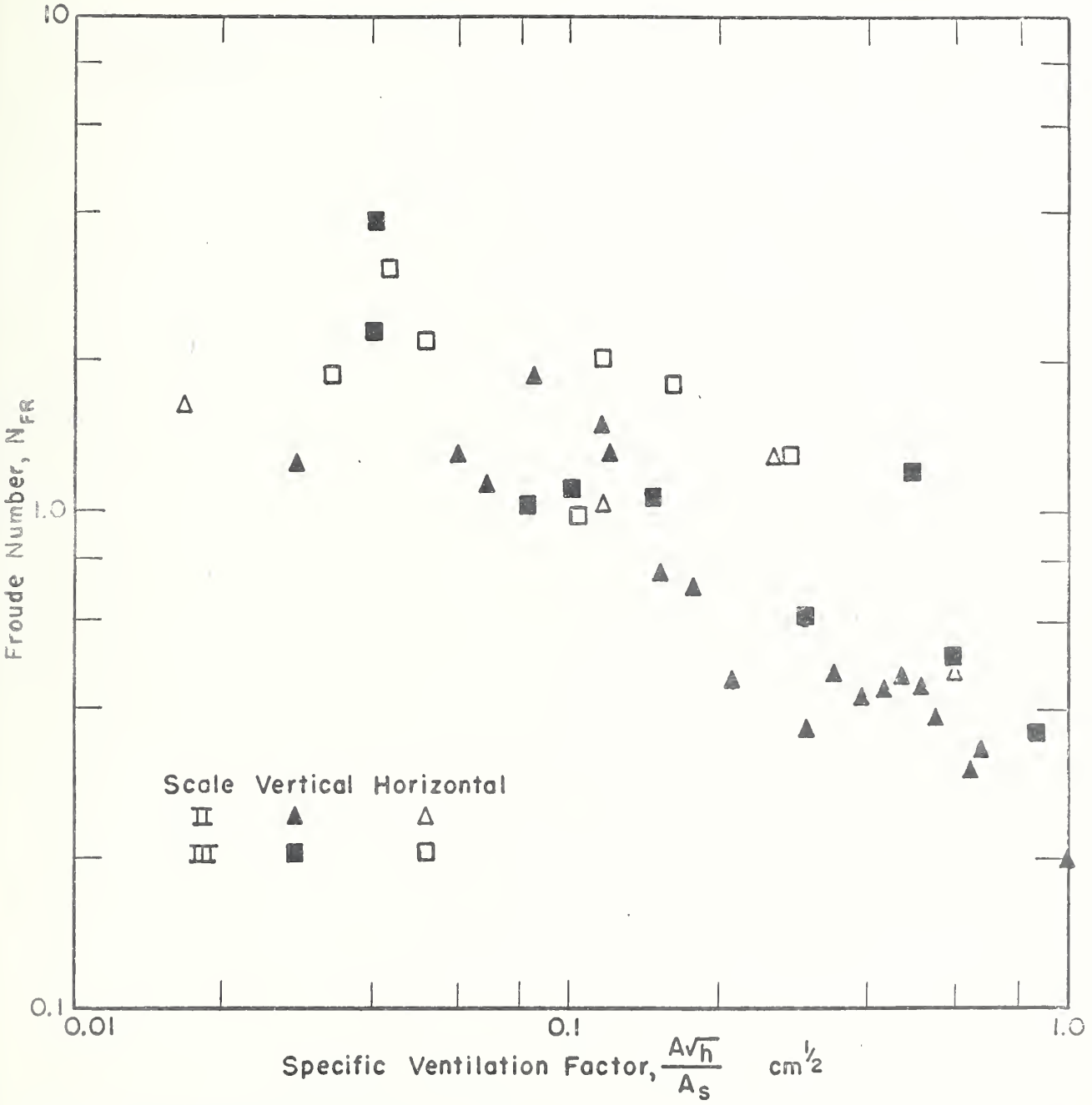

FIG. 14 – FROUDE NUMBER AND VENTILATION FACTOR FOR TWO ENCLOSURES

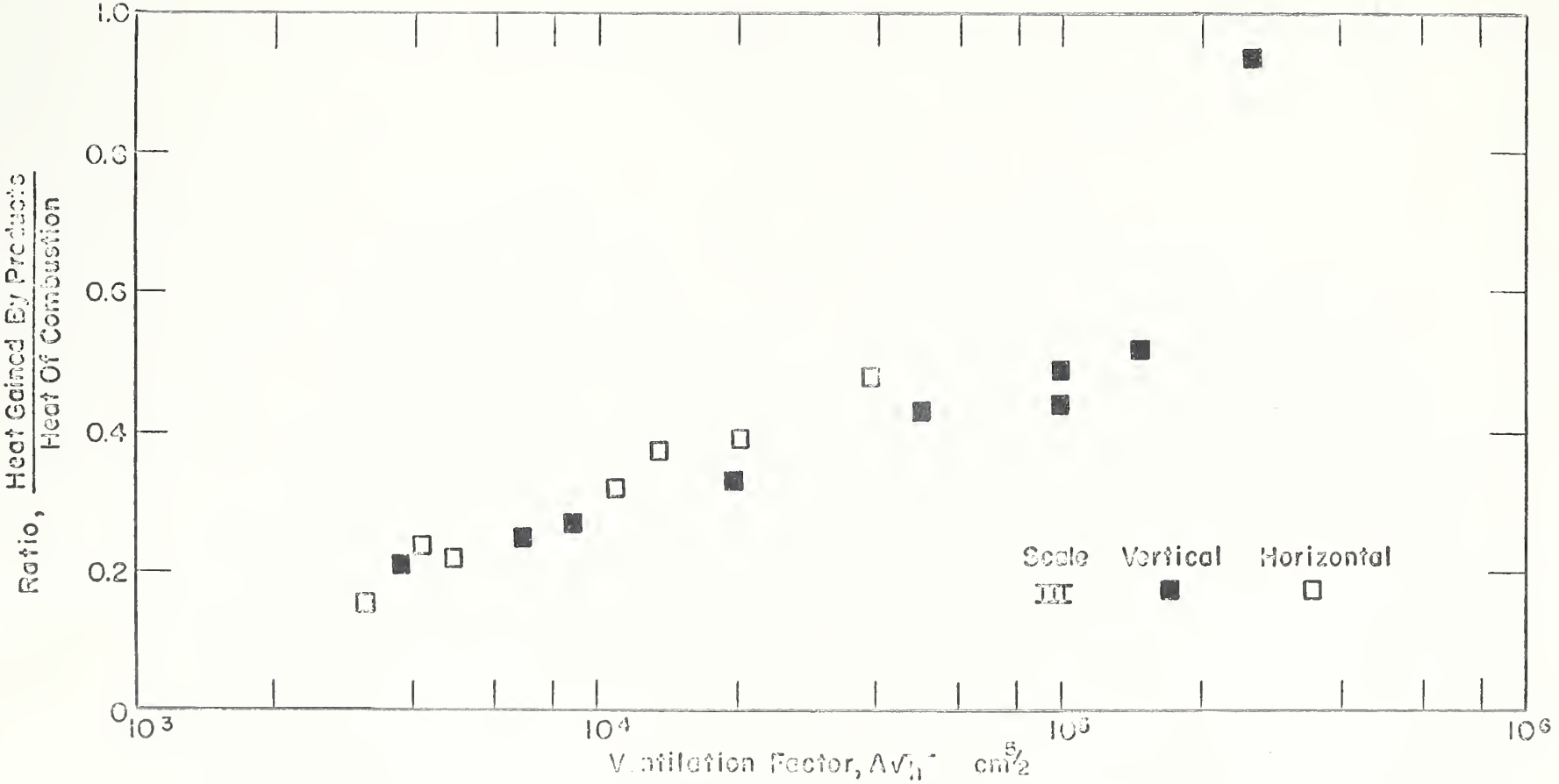

FIG.13—RELATIVE HEAT CONTENT OF EXHAUST GASES AND VENTILATION FACTOR
[illegible]


DEPARTMENT OF COMMERCE
NATIONAL BUREAU OF STANDARDS